

Solvent-Free Lanthanoid Complexes Derived From Chelation-Supported Organoamide Ligands^[‡]

Glen B. Deacon,^{*[a]} Craig M. Forsyth,^[a] and Natalie M. Scott^[a]

Keywords: N,O ligands / Lanthanides / Halides / Metathesis / Structure elucidation

Treatment of LnCl_3 with three molar equivalents of LiL [$\text{L} = N$ -(2-methoxyphenyl)- N -(trimethylsilyl)amide (L^1) or N -(2-phenoxyphenyl)- N -(trimethylsilyl)amide (L^2)], generated in situ from LH and $n\text{BuLi}$, or with the isolated lithium complex $[\text{Li}(\text{L}^1)(\text{OEt}_2)]_2$ (for $\text{Ln} = \text{Yb}$) in THF afforded the solvent-free homoleptic complexes $[\text{Ln}(\text{L})_3]$ [$\text{Ln} = \text{Yb}$ (**1a**), Er (**1b**), Sm (**1c**), Pr (**1d**), Nd (**1e**), $\text{L} = \text{L}^1$; $\text{Ln} = \text{Yb}$ (**2a**), Y (**2b**), Sm (**2c**), Nd (**2d**), La (**2e**), $\text{L} = \text{L}^2$]. With a 2:1 LiL (generated in situ) to LnCl_3 molar ratio, the solvent-free heteroleptic complexes $[\text{Ln}(\text{L})_2(\mu\text{-Cl})_2]$ were obtained for $\text{L} = N,N$ -dimethyl- N' -trimethylsilylethane-1,2-diaminate (en') [$\text{Ln} = \text{Yb}$ (**3a**), Er (**3b**), Sm (**3c**), Nd (**3d**), La (**3e**)], but not for L^1 or L^2 , which gave $[\text{Ln}(\text{L})_3]$ [$\text{Ln} = \text{Yb}$ (**1a**), Nd (**1e**), $\text{L} = \text{L}^1$; $\text{Ln} = \text{Yb}$ (**2a**), Nd (**2d**), La (**2e**), $\text{L} = \text{L}^2$]. However, treatment of LnCl_3 with two molar equivalents of the isolated crystalline lithium salt $[\text{Li}(\text{L}^1)(\text{OEt}_2)]_2$ in THF gave, for the heavier lanthanoids, the solvent-free heteroleptic complexes $[\text{Ln}(\text{L}^1)_2(\mu\text{-Cl})_2]$ [$\text{Ln} = \text{Yb}$ (**4a**), Er (**4b**), Tb (**4c**)], although the homoleptic complex $[\text{Nd}(\text{L}^1)_3]$ (**1e**)

was obtained for Nd. In contrast, similar reactions of isolated $[\text{Li}(\text{L}^2)(\text{DME})]$ with LnCl_3 yielded the heteroleptic species $[\text{Ln}(\text{L}^2)_2(\mu\text{-Cl})_2]$ only for $\text{Ln} = \text{Nd}$ [**5a**·(PhMe)₂]. At either end of the Ln series, the homoleptic $[\text{Ln}(\text{L}^2)_3]$ complexes [$\text{Ln} = \text{Yb}$ (**2a**), La (**2e**)] were obtained. Single crystal X-ray analyses of **1e** or **2a–2e** (as their PhMe or $\text{C}_5\text{H}_9\text{Me}$ solvates) showed these complexes to be monomeric and six-coordinate (*mer* isomer), whereas the heteroleptic complexes **4a–4c**, **5a** were found to be dimeric with bridging chloride atoms. Two chelating $[\text{L}^1]^-$ or $[\text{L}^2]^-$ units [*trans* O(Me/Ph) and *cis* amido groups] are bound to each lanthanoid centre completing a six-coordinate very distorted octahedral environment. The X-ray structure of $[\text{Li}(\text{L}^1)(\text{OEt}_2)]_2$ revealed a dimeric structure with each lithium four-coordinate and surrounded by one diethyl ether, two bridging amide nitrogens and a methoxy oxygen in a distorted tetrahedral array.

© Wiley-VCH Verlag GmbH, 69451 Weinheim, Germany, 2002

Introduction

The $6e^-$ donor cyclopentadienyl ligand (Cp) has been extensively used as a coligand with early transition metals for various types of catalytic transformations. Important applications include highly active group 4 and 5 metal and lanthanoid organometallic compounds in homogeneous Ziegler–Natta alkene polymerisation.^[2–7] In the last decade an increasing number of investigators have turned their attention away from cyclopentadienyl ligands to find alternative systems to stabilise the metal–carbon bond for catalytic work.^[7–9] Alternative systems using alkoxide and amide ligands in place of Cp have shown similar reaction chemistry with the stabilisation of early electron-deficient transition metals in medium to high oxidation states.^[6,7,9–14] Of these two alternatives, greater opportunities for substituent variation exist for the amide ligand. There are numerous N-containing ligands that can stabilise heteroleptic lanthanoid complexes, such as bis-

(trimethylsilyl)amide,^[15–18] benzamidinates,^[19–21] aminotropiminates^[22,23] and diazabutadienes.^[24] These bulky ligands can block coordination sites around the metal centre leading to monomeric, hydrocarbon soluble, electron-poor species that display unique chemical properties. However, in comparison to the stability offered by the cyclopentadienyl ligand in $[\text{Ln}(\text{Cp})_2(\text{X})]$ ($\text{X} = \text{anion}$), the labile nature of organoamide ligands in such systems has often caused ligand redistribution, resulting in the isolation of homoleptic derivatives.^[7,15,22,25,26] The incorporation of a supporting donor atom to give a bidentate amide ligand may improve the stability of the heteroleptic complexes. Encouragement for this idea came from the observation that N,N -dimethyl- N' -trimethylsilylethane-1,2-diaminate (en') gave not only the homoleptic complexes $[\text{Ln}(\text{en}')_3]$ ($\text{Ln} = \text{Lu}, \text{Er}, \text{Eu}, \text{Sm}, \text{Nd}, \text{La}$) but also a single example of a heteroleptic derivative $[\text{Er}(\text{en}')_2\text{Cl}]$.^[27] We now report a study of the use of the two new mixed N,O-donor bidentate amide ligands N -(2-methoxyphenyl)- N -(trimethylsilyl)amide (L^1)^[28] and N -(2-phenoxyphenyl)- N -(trimethylsilyl)amide (L^2)^[28,29] for preparing $[\text{Ln}(\text{L})_3]$ and $[\text{Ln}(\text{L})_2\text{Cl}]$ complexes, and extend the en' heteroleptic series to lanthanoids other than Er. Previous studies on lanthanoid complexes containing the L^1 and L^2 ligands have shown them to be capable of supporting

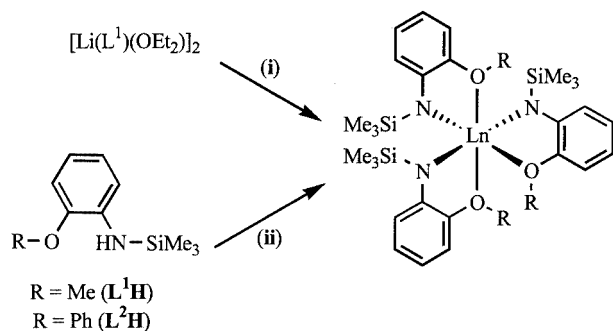
[‡] Organoamido- and Aryloxo-Lanthanoids, 28. Part 27: see Ref.^[1]

[a] School of Chemistry, Monash University, 3800 Victoria, Australia
E-mail: glen.deacon@sci.monash.edu.au

organo-oxo heteroleptic complexes viz. $[\text{Yb}(\text{L}^1)_2(\mu\text{-OMe})_2]$ and $[\text{Yb}(\text{L}^2)_2(\text{OPh})(\text{THF})]$ (THF = tetrahydrofuran).^[28]

Results and Discussion

A range of $[\text{Ln}(\text{L})_3]$ complexes [$\text{L} = \text{L}^1$, $\text{Ln} = \text{Yb}$ (**1a**), Er (**1b**), Sm (**1c**), Pr (**1d**), Nd (**1e**); $\text{L} = \text{L}^2$, $\text{Ln} = \text{Yb}$ (**2a**), Y (**2b**), Sm (**2c**), Nd (**2d**), La (**2e**)] were prepared by treatment of LnCl_3 with three molar equivalents of LiL as the isolated $[\text{Li}(\text{L}^1)(\text{OEt}_2)_2]$ [Scheme 1 (i)] or generated in situ from the reaction of LH with $n\text{BuLi}$ in THF [Scheme 1 (ii)]. The crystalline complexes $[\text{Ln}(\text{L}^1)_3]$ [$\text{Ln} = \text{Yb}$ (**1a**), Er (**1b**), Sm (**1c**), Pr (**1d**), Nd (**1e**)] were isolated from hexane in good yield after removal of the precipitated LiCl . The $[\text{Ln}(\text{L}^2)_3]$ complexes [$\text{Ln} = \text{2a} \cdot (\text{PhMe})$, $\text{2a} \cdot (\text{C}_5\text{H}_9\text{Me})$] (from a 1:2 mol ratio synthesis – see below), $\text{2b} \cdot (\text{C}_5\text{H}_9\text{Me})$, $\text{2c} \cdot (\text{PhMe})$, $\text{2d} \cdot (\text{PhMe})_2$, $\text{2e} \cdot (\text{PhMe})$] were obtained by crystallisation of the bulk products from toluene. Whilst toluene solvates are not unusual, the isolation of methylcyclopentane solvates (as identified from X-ray crystallography) was unexpected. The latter are presumed to be derived from a trace impurity in one of the solvents (PhMe or hexane) used. Crystallisation of $\text{2e} \cdot (\text{PhMe})$ from diethyl ether gave $[\text{La}(\text{L}^2)_3]$ (**2e**), which was used for an X-ray determination, whilst single crystals of solvent-free $[\text{Nd}(\text{L}^2)_3]$ (**2d**) were obtained by crystallisation of $\text{2d} \cdot (\text{PhMe})_2$ from hexane.



Scheme 1. Reagents and conditions: (i) THF , 0.33 equivalents of YbCl_3 followed by crystallisation from hexane (**1a**); (ii) $n\text{BuLi}$, THF , 0°C , 0.33 equivalents of LnCl_3 followed by crystallisation from hexane (**1b**–**1e**) or toluene (**2a**·(PhMe), **2a**·($\text{C}_5\text{H}_9\text{Me}$)) (0.50 equivalents of YbCl_3), **2b**·($\text{C}_5\text{H}_9\text{Me}$), **2c**·(PhMe), **2d**·(PhMe)₂, **2e**·(PhMe)

Satisfactory elemental analyses (C, H N) were obtained for all of the homoleptic complexes although crystallographically characterised unsolvated **2e** was not examined as the corresponding toluene solvate was obtained analytically pure. In the case of **2a**·($\text{C}_5\text{H}_9\text{Me}$) the analysis fitted for solvent-free $[\text{Yb}(\text{L}^2)_3]$ hence the methylcyclopentane was evidently removed from the lattice on drying the sample under vacuum. The corresponding undried yttrium complex analysed as the solvate. The infrared spectra of the complexes were virtually identical within each series and indicated the presence of coordinated L^1 or L^2 in accordance with the proposed compositions. For **2a**·(PhMe), **2c**·(PhMe), **2d**·(PhMe)₂ and **2e**·(PhMe) the presence of toluene could not be detected by infrared spectroscopy due to

the large number of ligand bands. Asymmetric C–O–C stretching for $[\text{Ln}(\text{L}^1)_3]$ [$\text{Ln} = \text{Yb}$ (**1a**), Er (**1b**), Sm (**1c**), Pr (**1d**), Nd (**1e**)] gives two sets of two bands while for L^1H only one set is observed.^[28] For $[\text{Ln}(\text{L}^2)_3]$ [$\text{Ln} = \text{Yb}$ {**2a**·(PhMe), **2a**·($\text{C}_5\text{H}_9\text{Me}$)}, Y {**2b**·($\text{C}_5\text{H}_9\text{Me}$)}, Sm {**2c**·(PhMe)}, Nd {**2d**·(PhMe)₂}, La {**2e**·(PhMe)}] this region displays three sets of two absorptions. This feature is different from the behaviour of L^2H , which displays only two sets of two absorptions in this region.^[28] Generally, the ^1H NMR spectroscopic data for **1e**, **2b**·($\text{C}_5\text{H}_9\text{Me}$), **2c**·(PhMe), **2d**·(PhMe)₂, **2e**·(PhMe) and **2e** indicate that one L environment is present in solution, in contrast to the two L environments observed in the solid state (see below). Presumably the ligands are rapidly exchanging under these conditions. Characteristic toluene resonances were observed for the **2c**–**2e**·(PhMe)_n complexes and confirmed the number of toluene molecules of crystallisation per $[\text{LnL}_3]$ indicated by microanalysis. For **2b**·($\text{C}_5\text{H}_9\text{Me}$) the ^1H NMR spectrum is consistent with the presence of methylcyclopentane,^[30] although the integration indicated only half a methylcyclopentane molecule per $[\text{Y}(\text{L}^2)_3]$. However, the X-ray structure determination and elemental analyses indicated one $\text{C}_5\text{H}_9\text{Me}$ per yttrium. Whilst the ^1H NMR spectrum of **1e** is similar to that of **2d**·(PhMe)₂ for structurally common protons, the paramagnetic behaviour of Nd^{3+} causes most backbone aromatic resonances on L^1 or L^2 to shift considerably from those of diamagnetic **2e** (see Exp. Sect.). In the mass spectra of **1c** and **1e**, the highest metal-containing fragment was attributable to the parent ion $[\text{Ln}(\text{L}^1)_3]^+$; loss of the groups SiMe_3 and OMe or OPh from the molecular ion was observed for **1b**, **2a**·(PhMe) or **2a**·($\text{C}_5\text{H}_9\text{Me}$). The mass fragment $[\text{Ln}(\text{L}^1)_2]^+$ was observed in the spectra of all three complexes, as well as the metal-free fragment $[\text{L}^1\text{H}]^+$. The mass spectra of **2b**·($\text{C}_5\text{H}_9\text{Me}$) and **2c**·(PhMe) showed a weak molecular ion $[\text{Ln}(\text{L}^2)_3]^+$ and associated fragment ions (notably $[\text{Ln}(\text{L}^2)_2]^+$ and $[\text{Ln}(\text{L}^2)]^+$) as well as an intense $[\text{L}^2\text{H}]^+$ ion. However for **2e**·(PhMe) the highest mass ion observed was $[\text{La}(\text{L}^2)_2]^+$. The UV/Vis/NIR spectrum of a solution of **1a** in DME exhibited absorptions characteristic of $f \leftarrow f$ transitions of the Yb^{3+} cation^[31] near 1000 nm.

Single crystal X-ray diffraction data were collected for **1e** (Figure 1), **2a**·(PhMe) (Figure 2), **2d** and **2e**. Data were also obtained for **2a**·($\text{C}_5\text{H}_9\text{Me}$) and **2b**·($\text{C}_5\text{H}_9\text{Me}$) and have been deposited with the Cambridge Crystallographic Data Centre (CCDC-174206/7). Selected bond lengths and angles for **1e**, **2a**·(PhMe), **2b**·($\text{C}_5\text{H}_9\text{Me}$), **2d** and **2e** are given in Table 1. Each of the molecules is monomeric with a six-coordinate metal centre surrounded by three bidentate L ligands ($\text{L} = \text{L}^1$ or L^2) with the bulky amido groups arranged in a *meridional* configuration. The geometry is best described as a distorted octahedron (best-fit polyhedron^[32]) with the oxygen atoms [O(1) and O(3)], nitrogen atoms [N(1) and N(2)], and the other donor pair [O(2) and N(3)] occupying *transoid* sites. The *mer* arrangement of the L^1 or L^2 ligands differs from that of the closely related complex $[\text{Ln}(\text{en}')_3]$ ($\text{en}' = N,N$ -dimethyl- N' -trimethylsilylethane-1,2-diaminate)^[27] which has a *fac* orientation of the bidentate

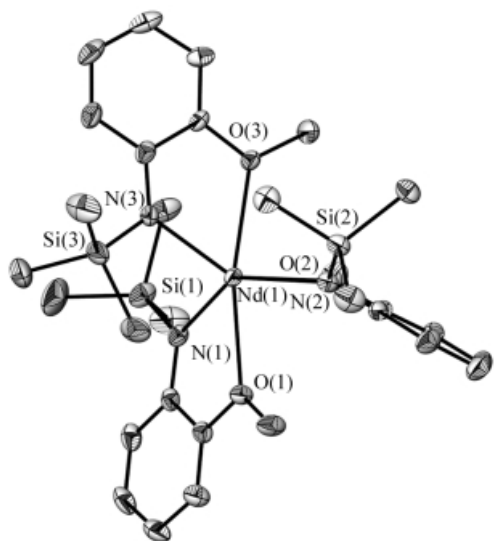


Figure 1. ORTEP view of $[\text{Nd}(\text{L}^1)_3]$ (**1e**) drawn with 50% ellipsoids; hydrogen atoms have been omitted for clarity

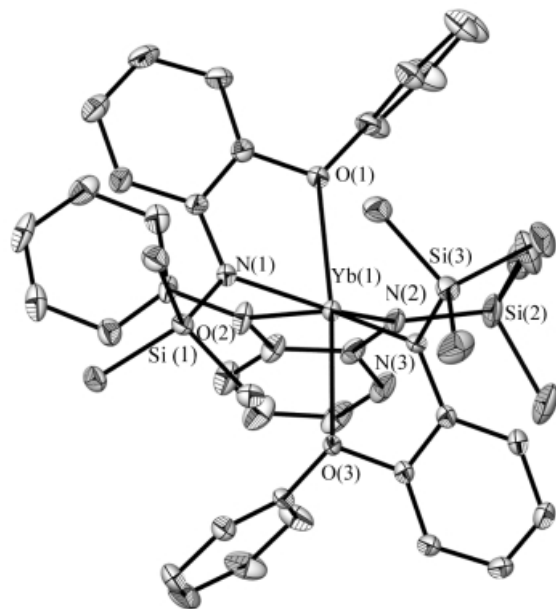


Figure 2. ORTEP view of $[\text{Yb}(\text{L}^2)_3] \cdot (\text{PhMe})$ (**2a**·PhMe) drawn with 50% ellipsoids; hydrogen atoms and toluene of crystallisation have been omitted for clarity

en' amide ligands. The latter was unexpected since the very bulky NSiMe_3 groups are all in a *cis* disposition. Thus the $\text{N}-\text{Ln}-\text{N}$ angles lie in the range $[104.8(5)-109.0(1)^\circ]$ for $[\text{Ln}(\text{en}')_3]$ ($\text{Ln} = \text{Lu}, \text{Er}, \text{Eu}$)^[27] whereas **1e**, **2a**·PhMe, **2d** and **2e** have two similar angles but one larger *transoid* angle (Table 1). Even with the *mer* configuration, two of the NSiMe_3 groups are pushed above and below the equatorial plane presumably to reduce steric repulsion from the otherwise closely proximate bulky amides. The less sterically dominating $\text{O}(\text{Me}/\text{Ph})$ groups occupy the *trans* sites with $\text{O}(1)-\text{Ln}(1)-\text{O}(3)$ angles verging on linear, although the angles between the remaining *transoid* donors $\text{N}(1)-\text{Ln}-\text{N}(2)$ and $\text{N}(3)-\text{Ln}-\text{O}(2)$ are significantly less

than 180° . This is presumably due to a combination of the small bite angle of the chelated L^1 or L^2 ligands and the proximity of the *cis* amide groups.

The geometry of $[\text{Nd}(\text{L}^2)_3]$ is almost identical to that of $[\text{Nd}(\text{L}^1)_3]$ with the angles defining the coordinated atoms differing by less than 10° (Table 1). Whilst the general appearance of the $[\text{Ln}(\text{L}^2)_3]$ complexes is the same, significant differences are apparent between the solvated and solvent-free structures. The *trans* $\text{N}-\text{Ln}-\text{N}$ angles for unsolvated **2d** and **2e** are approximately 12° smaller than those for **2a**·PhMe and **2b**· $\text{C}_5\text{H}_9\text{Me}$, and a similar, but less marked, trend is also observed for the *cis* $\text{N}-\text{Ln}-\text{N}$ angles (Table 1). Thus the solvates are closer to a regular octahedral structure. These differences are clearly not due to the gradual change in ionic radii from La (1.03 Å) to Yb (0.87 Å).^[33] For example, the smaller elements would be expected to be more sterically crowded causing a widening of the *cis* $\text{N}-\text{Ln}-\text{N}$ angles through greater repulsion between the bulky SiMe_3 groups. In fact the opposite is observed. However, the *cis* $\text{N}-\text{Ln}-\text{N}$ angles are not unreasonably narrow and still compare well with those of *fac*- $[\text{Ln}(\text{en}')_3]$.^[27] Therefore the variation in angles is possibly associated with differences in the crystal packing required to accommodate solvent molecules.

A comparison of the metal-nitrogen distances with those of other lanthanoid organoamides can be made by subtraction of the appropriate metal ionic radius (Table 2).^[33] Selected examples from the literature are listed in Table 2 and the values derived for the current $[\text{Ln}(\text{L})_3]$ complexes (L^1 : 1.37–1.40 Å, L^2 : 1.36–1.43 Å) lie near the middle of the observed range (1.34–1.49 Å) and are therefore not unusual. For **1e**, **2a**·PhMe and **2b**· $\text{C}_5\text{H}_9\text{Me}$ there is some variation in the $\text{Ln}-\text{N}$ distances with one shorter $[\text{Ln}(1)-\text{N}(3)]$ and two longer bonds, whereas the three $\text{Ln}(1)-\text{N}(\text{amide})$ bond lengths of **2d** and **2e** are very similar (Table 1). Whilst bond lengthening of the mutually *trans* amides might be expected, this is not observed for any of the complexes. Perhaps the inconsistently shorter $\text{Ln}-\text{N}(3)$ distance reflects extraneous factors, for example packing forces. Subtraction values derived from the $\text{Ln}-\text{O}$ distances (1.48–1.60 Å) are significantly longer than those derived from organolanthanoid or halolanthanoid ether complexes $[\text{LnR}_3(\text{ether})_n]$: 1.34 ± 0.05 Å;^[34] $\text{LnX}_3(\text{THF})_n$: 1.39–1.44 Å^[35] but the $\text{Nd}-\text{O}$ distances are shorter than those $[2.614(4)-2.740(4)$ Å] in the related neodymium bidentate amide complex $[\text{Nd}\{\text{Me}_2\text{Si}(\text{O}t\text{Bu})(\text{N}t\text{Bu})\}_3]$.^[36] The ether fragments of $[\text{Nd}\{\text{Me}_2\text{Si}(\text{O}t\text{Bu})(\text{N}t\text{Bu})\}_3]$ and $[\text{Ln}(\text{L})_3]$ are bulkier than a simple ether ligand such as THF, and this may account for the long $\text{Ln}-\text{O}$ distances, although the bond lengthening may also be an indication of general steric crowding in these complexes. The contraction of the subtraction values for the $\text{Ln}-\text{O}(\text{Ph})$ bonds from La to Yb in the $[\text{Ln}(\text{L}^2)_3]/[\text{Ln}(\text{L}^2)_3] \cdot \text{S}_n$ complexes (Table 2) is contrary to the expected trend since the increase in steric crowding associated with the smaller size of the metal centre may result in metal-oxygen bond lengthening. Since there are two distinct groups of data corresponding to the presence or absence of a solvent of crystallisation, these variations in

Table 1. Metal atom environments for [Ln(L)₃] complexes

	[Nd(L ¹) ₃] 1e	[Yb(L ²) ₃](PhMe) 2a (PhMe)	[Y(L ²) ₃](C ₅ H ₉ Me) 2b (C ₅ H ₉ Me) ^[a]	[Nd(L ²) ₃] 2d	[La(L ²) ₃] 2e
Bond length (Å)					
Ln(1)–N(1)	2.385(3)	2.272(2)	2.306(3)	2.396(2)	2.454(2)
Ln(1)–N(2)	2.376(3)	2.289(3)	2.331(3)	2.387(2)	2.447(2)
Ln(1)–N(3)	2.349(3)	2.231(3)	2.270(3)	2.386(2)	2.446(2)
Average	2.37	2.26	2.30	2.39	2.45
Ln(1)–O(1)	2.534(2)	2.350(3)	2.381(2)	2.550(2)	2.609(1)
Ln(1)–O(2)	2.535(2)	2.359(3)	2.441(2)	2.543(2)	2.606(2)
Ln(1)–O(3)	2.536(2)	2.405(3)	2.386(2)	2.575(1)	2.633(1)
Average	2.54	2.37	2.40	2.56	2.62
Angles (°)					
N(1)–Ln(1)–N(2)	139.63(9)	150.10(10)	148.15(10)	136.05(6)	134.17(5)
N(1)–Ln(1)–N(3)	98.82(9)	104.40(10)	105.71(10)	107.77(6)	109.22(5)
N(2)–Ln(1)–N(3)	119.23(9)	105.298(10)	106.01(10)	115.47(6)	116.09(5)
N(1)–Ln(1)–O(1)	65.62(8)	71.37(8)	70.33(9)	66.32(5)	64.65(5)
N(2)–Ln(1)–O(2)	66.12(8)	69.39(9)	68.37(9)	65.95(5)	64.19(5)
N(3)–Ln(1)–O(3)	65.38(8)	72.16(8)	71.02(9)	65.51(5)	63.82(5)
O(1)–Ln(1)–O(2)	88.48(7)	86.56(8)	85.63(8)	86.02(5)	85.43(5)
O(1)–Ln(1)–O(3)	167.65(7)	174.55(7)	174.28(7)	168.08(5)	168.26(4)
O(2)–Ln(1)–O(3)	82.42(7)	90.06(8)	89.97(8)	83.28(5)	83.78(5)
O(1)–Ln(1)–N(2)	80.87(8)	94.39(9)	94.23(9)	82.08(6)	82.32(5)
O(1)–Ln(1)–N(3)	124.75(8)	111.47(9)	113.58(9)	125.49(6)	127.19(5)
O(2)–Ln(1)–N(1)	90.19(8)	83.30(9)	82.44(9)	81.51(5)	81.56(5)
O(2)–Ln(1)–N(3)	146.38(8)	161.78(8)	160.63(9)	148.44(5)	147.35(5)
O(3)–Ln(1)–N(1)	122.48(8)	104.00(8)	105.48(9)	116.96(5)	118.06(5)
O(3)–Ln(1)–N(2)	87.79(8)	88.41(9)	87.54(9)	88.75(5)	88.81(5)

^[a] Crystallographic data for **2a**(C₅H₉Me) in CCDC-174206.

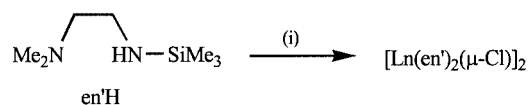
Table 2. Subtraction values from Ln–N, O, Cl distances for a selection of organoamidolanthanoid complexes

Compound	Ref	Coordination number	Av. Ln–N length [d(N)] Å	Av. Ln–O length [d(O)] Å	Ionic Radii of Ln ³⁺ (ir) Å ^[a]	d(N)–ir (Å)	d(O)–ir (Å)
[Nd(L ¹) ₃] (1e)	This work	6	2.37	2.54	0.98	1.39	1.56
[Yb(L ²) ₃](PhMe) [2a (PhMe)]	This work	6	2.26	2.37	0.87	1.39	1.50
[Nd(L ²) ₃] (2d)	This work	6	2.39	2.56	0.98	1.41	1.58
[La(L ²) ₃] (2e)	This work	6	2.45	2.62	1.03	1.42	1.59
[Y(L ²) ₃](C ₅ H ₉ Me) [2b (C ₅ H ₉ Me)]	This work	6	2.30	2.40	0.90	1.40	1.50
[Nd{N(SiMe ₃) ₂ }] ₃	[37]	3	2.29		0.82 ^[b]	1.47	
[Eu{N(SiMe ₃) ₂ }] ₃	[38]	3	2.26		0.78 ^[b]	1.48	
[Yb{N(SiMe ₃) ₂ }] ₃	[38]	3	2.16		0.71 ^[b]	1.45	
[Nd{N(Ph)(SiMe ₃) ₂ }] ₃ (THF)	[39]	4	2.31		0.88 ^[b]	1.43	
[Yb{NH(2,6- <i>iPr</i>) ₂ C ₆ H ₃ }] ₃ (THF) ₂	[11]	5	2.17		0.82 ^[b]	1.35	
[Sm{N(Cy) ₂ }] ₃ (THF) ^[c]	[40]	4	2.28		0.90 ^[b]	1.38	
[Eu(en) ₃]	[27]	6	2.29		0.95	1.34	
[Er(en) ₃]	[27]	6	2.24		0.89	1.35	
[Lu(en) ₃]	[27]	6	2.19		0.86	1.33	
[Nd{Me ₂ Si(OrBu)(<i>n</i> Bu)} ₃]	[36]	6	2.40	2.68	0.98	1.42	1.70
[Pr{4-MeOC ₆ H ₄ C(NSiMe ₃) ₂ }] ₃	[41]	6	2.48		0.99	1.49	
				Av. Ln–Cl length [d(Cl)] Å			d(Cl)–ir (Å)
[Ln(L ¹) ₂ (μ-Cl)] ₂ [Ln = Yb (4a), Tb (4b), Er (4c)]	This work	6	2.19–2.26	2.68–2.74	0.92, 0.89, 0.87	1.32–1.34	1.79–1.83
[Nd(L ²) ₂ (μ-Cl)] ₂ (PhMe) ₂ [5a (PhMe) ₂]	This work	6	2.32, 2.30	2.79, 2.86	0.98	1.32, 1.34	1.80, 1.87
[Nd{N(2,6- <i>iPr</i>) ₂ C ₆ H ₃ }(SiMe ₃) ₂ }] ₂ (THF)(μ-Cl) ₂ Li(THF) ₂	[39]	5	2.30	2.76	0.92 ^[b]	1.38	1.84
[Sm{N(SiMe ₃) ₂ }] ₂ (μ-Cl)(THF) ₂	[17]	5	2.27	2.78	0.90 ^[b]	1.37	1.88
[Gd{N(SiMe ₃) ₂ }] ₂ (μ-Cl)(THF) ₂	[15]	5	2.25	2.75	0.89 ^[b]	1.36	1.86
[Yb{N(SiMe ₃) ₂ }] ₂ (μ-Cl)(THF) ₂	[15]	5	2.19	2.68	0.82 ^[b]	1.37	1.86
[Sm{N(Cy) ₂ }] ₂ (μ-Cl)(THF) ₂ ^[c]	[40]	5	2.21	2.80	0.90 ^[b]	1.31	1.90
[Nd{(CF ₃) ₂ C ₆ H ₃ C(NSiMe ₃) ₂ }] ₂ (μ-Cl) ₂ Li(THF) ₂	[42]	6	2.53	2.71	0.98	1.55	1.73
[Sm{Li(<i>t</i> BuDAB)} ₂ (THF)] ₂ (μ-Cl) ₂ Li(THF) ₂ ^[d]	[25]	8	2.45	2.88	1.08	1.37	1.80
[Yb{Me ₂ Si(OrBu)(<i>n</i> Bu)} ₂ (μ-Cl) ₂ Li(THF) ₂]	[36]	6	2.24	2.64	0.87	1.37	1.77
[Er{(iPr)TP}(μ-Cl)] ₂ ^[e]	[23]	6	2.32	2.73	0.89	1.44	1.84
[Yb{(iPr)TP}(μ-Cl)] ₂ ^[e]	[23]	6	2.30	2.71	0.87	1.43	1.84
[Y(η ⁵ -η ¹ -C ₅ Me ₄ SiMe ₂ NCMe ₂ Et)(THF)(μ-Cl)] ₂	[43]	7	2.24	2.74	0.96	1.28	1.78
[Yb(η ⁵ -C ₅ H ₅)(μ-Cl)] ₂	[44]	8	–	2.64	0.98	–	1.66
[Lu(η ⁵ -C ₅ H ₅ SiMe ₃) ₂ (μ-Cl)] ₂	[45]	8	–	2.62	0.98	–	1.64
[Sm(η ⁵ -C ₅ Me ₅)(μ-Cl)] ₃	[46]	8	–	2.88	1.08	–	1.80
[Yb(Cl) ₂ (μ-Cl)(THF) ₂] ^[f]	[47]	6	–	2.68	0.87	–	1.81

^[a] Values derived from R. D. Shannon.^[33] ^[b] Numbers extrapolated from values of higher coordination number from ^[a]. ^[c] Cy = cyclohexyl. ^[d] *t*BuDAB = di-*tert*-butyl-1,4-diazabutadiene. ^[e] [(*i*Pr)TP]²⁻ = 1,3-bis[2-(isopropylamino)troponiminato]propane. ^[f] Value of the Yb–μ-Cl distance only.

bond lengths and angles may be a result of a packing effect resulting from the presence or absence of the solvent.

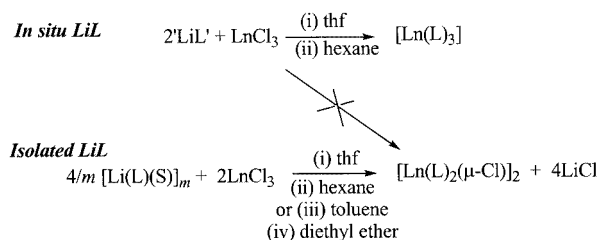
With successful coordination of bidentate organoamide ligands [not only in the current examples, but also the previously reported $[\text{Ln}(\text{en}')_3]$ complexes ($\text{Ln} = \text{Lu}, \text{Er}, \text{Eu}, \text{Sm}, \text{Nd}, \text{La}$)],^[27] the next challenge was to prepare heteroleptic chloride species of the type $[\text{Ln}(\text{L})_2\text{Cl}]$. Such complexes are pivotal intermediates for the generation of catalytically active materials.^[4,5,7] A one-pot reaction was initially reported^[27] to be successful for the en' ligand, yielding one example of the target molecules, $[\text{Er}(\text{en}')_2\text{Cl}]$. This has now been shown to be general across the lanthanoid series with the preparation of the heteroleptic diorganoamidolanthanoid complexes $[\text{Ln}(\text{en}')_2(\mu\text{-Cl})_2]$ [$\text{Ln} = \text{Yb}$ (**3a**), Er (**3b**), Sm (**3c**), Nd (**3d**) and La (**3e**)] (Scheme 2). The lanthanoid products were very soluble in hydrocarbon solvents and were crystallised with difficulty from concentrated solutions at -20°C . Furthermore, the removal of LiCl from the reaction mixture was tedious with numerous low temperature extractions required in order to obtain pure $[\text{Ln}(\text{en}')_2(\mu\text{-Cl})_2]$ derivatives, which were subsequently isolated in only low to moderate yields.



Scheme 2. Reagents and Conditions; (i) $n\text{BuLi}$, THF, 0°C , then 0.5 equivalents of LnCl_3 ($\text{Ln} = \text{Yb}, \text{Er}, \text{Sm}, \text{Nd}, \text{La}$) followed by crystallisation from hexane

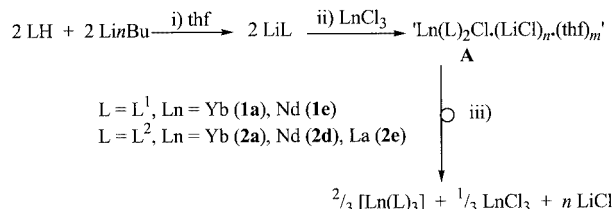
The addition of LnCl_3 to two molar equivalents of LiL ($\text{L} = \text{L}^1, \text{Ln} = \text{Yb}, \text{Nd}$; $\text{L} = \text{L}^2, \text{Ln} = \text{Yb}, \text{Nd}, \text{La}$), which was generated in situ in THF, resulted in complete dissolution of the starting materials. Extraction of the evaporated reaction mixtures with hexane gave the homoleptic complexes $[\text{Ln}(\text{L})_3]$ [$\text{L} = \text{L}^1, \text{Ln} = \text{Yb}$ (**1a**), Nd (**1e**); $\text{L} = \text{L}^2, \text{Ln} = \text{Yb}$ (**2a**·($\text{C}_5\text{H}_9\text{Me}$)) (from toluene/hexane), Nd (**2d**), La (**2e**)] instead of the target heteroleptic complexes $[\text{Ln}(\text{L})_2\text{Cl}]$ (Scheme 3). Subsequently, reactions using isolated crystalline lithium salts of L^1 and L^2 , such as dimeric $[\text{Li}(\text{L}^1)(\text{OEt}_2)]_2$ (below) or monomeric $[\text{Li}(\text{L}^2)(\text{DME})]$,^[29] with a variety of LnCl_3 compounds in a 2:1 Li to LnCl_3 mol ratio, were found to give LnL_2Cl complexes [$\text{L} = \text{L}^1, \text{Ln} = \text{Yb}$ (**4a**), Er (**4b**), Tb (**4c**); $\text{L} = \text{L}^2, \text{Ln} = \text{Nd}$ {**5a**·(PhMe)₂}] (Scheme 3). Typically, hexane extraction was employed for the isolation of $[\text{Ln}(\text{L}^1)_2(\mu\text{-Cl})_2]$ (**4a–4c**) species whilst toluene was used for **5a**·(PhMe)₂ (Scheme 3). However, the isolation of the homoleptic products **2a** and **2e** from reactions of LnCl_3 with two equivalents of $[\text{Li}(\text{L}^2)(\text{DME})]$ ^[29] was also observed. Thus these results show that for L^1 and L^2 there is only a narrow window of opportunity to prepare the heteroleptic chlorides. Access to complexes of the smaller lanthanoid elements Tb, Er and Yb is available with L^1 , but the larger neodymium gives $[\text{Nd}(\text{L}^1)_3]$ (**1e**) whilst L^2 yields the heteroleptic derivative for the larger Nd but not with the lighter (La) and heavier (Yb) extremes of the lanthanoid series. These results support the view of Lappert et al. that fully characterised isolated lithium complexes are

more rewarding synthetically than reagents generated in situ.^[48,49] The synthetic value of *pre-isolated* alkali metal alkyls has been demonstrated in routes to ytterbium(II) alkyls.^[50]



Scheme 3. Reagents and Conditions; In situ 'LiL'; (ii) $\text{L} = \text{L}^1, \text{Ln} = \text{Yb}$ (**1a**), Nd (**1e**); $\text{L} = \text{L}^2, \text{Ln} = \text{Yb}$ (**2a**) (crystallised from toluene/hexane), Nd (**2d**), La (**2e**). Isolated LiL; (ii) $\text{L} = \text{L}^1, \text{Ln} = \text{Yb}, \text{Er}, \text{Tb}$, target **4a–4c** obtained; $\text{Ln} = \text{Nd}$ gives **1e**; (iii) $\text{L} = \text{L}^2, \text{Ln} = \text{Nd}$, **5a**·(PhMe)₂ obtained; $\text{Ln} = \text{Yb}, \text{La}$ afforded **2a, 2e**; ($\text{L} = \text{L}^2, \text{Ln} = \text{La}$, **2e** obtained

The direct formation of $[\text{Ln}(\text{L})_3]$ from a 2:1 (Li:Ln) reaction in THF would leave 0.33 equivalents of LnCl_3 unchanged, and lanthanoid halides have low solubility in this solvent. Since all the LnCl_3 dissolved, it suggests that the heteroleptic species is formed initially, possibly stabilised as an "ate" complex such as **A** in Scheme 4. The formation of "ate" complexes has previously been observed for other bulky organoamidolanthanoids, for example $[\text{Yb}\{\text{Me}_2\text{Si}(\text{O}t\text{Bu})(\text{N}t\text{Bu})\}_2(\mu\text{-Cl})_2\text{Li}(\text{THF})_2]$ ^[36] and $[\text{Nd}\{(\text{CF}_3)_3\text{C}_6\text{H}_2\text{C}(\text{NSiMe}_3)_2\}(\mu\text{-Cl})_2\text{Li}(\text{THF})_2]$.^[42] Therefore the rearrangement presumably occurs on addition of hexane [or for $\text{L}^2, \text{Ln} = \text{Yb}$, toluene (even with isolated LiL^2); for $\text{Ln} = \text{La}$, also diethyl ether; Scheme 4 (iii)] with precipitation of LiCl and LnCl_3 or even LiLnCl_4 . This is contrary to the in situ $[\text{Ln}(\text{en}')_2(\mu\text{-Cl})_2]$ preparations where the heteroleptic derivatives were obtained from hexane. Crystallisation of the "ate" complexes (**A** in Scheme 4) was unsuccessful due to the very high solubility of the reaction products. The reasons for the difference in outcome between the use of isolated and in situ formed LiL in two cases ($\text{L} = \text{L}^1, \text{Ln} = \text{Yb}$; $\text{L} = \text{L}^2, \text{Ln} = \text{Nd}$) are not clear but plausibly the in situ reagents are less pure.



Scheme 4. Postulated rearrangement pathway

Elemental analyses (C, H, N and/or Ln) for the $[\text{Ln}(\text{L})_2(\mu\text{-Cl})_2]$ complexes (except unanalysed **3b, 3c**) were consistent with the proposed formulations and the absence of coordinated THF. For each ligand type the infrared spectra of the $[\text{Ln}(\text{L})_2(\mu\text{-Cl})_2]$ complexes were almost identical, showing peaks attributable to the appropriate ligand and no evidence of THF. The spectra of **3a–3e** were very similar to those of the corresponding homoleptic species. In contrast

intense infrared absorptions of **4a–4c** attributable to C–O–C stretching of the MeOAr substituent were observed as two single bands at 1100–1000 cm^{-1} , whereas for *mer*-[Ln(L¹)₃] two bands were observed in each region. This may reflect the solely *trans* ether groups in **4a–4c** (below), whereas [Ln(L¹)₃] complexes have both *cis* and *trans* (Me)O–Ln–O(Me) arrays. Bands at 1266 and 859 cm^{-1} were observed for **5a**·(PhMe)₂ but not for **2d**·(PhMe)₂, and a band of the latter at 802 cm^{-1} was absent in the former, thereby distinguishing the spectra of the two complexes. Despite the paramagnetism of **5a**·(PhMe)₂, ¹H NMR resonances attributable to the L² ligand could be assigned (see Exp. Sect.), whilst those of toluene were in the usual diamagnetic region; integrations confirmed the proposed composition. Only a single L² environment was detected — consistent with the single type of L² coordination in the solid-state structure (below) — and the general spectral features were similar to those of **2d**·(PhMe)₂. The visible/near infrared spectrum of **5a**·(PhMe)₂ showed absorptions characteristic of Nd³⁺.^[31] Mass spectra identified a bimolecular species to be present for **3a–3e** with the highest-mass fragment, except for ytterbium, being the ion [Ln₂(en')₃Cl₂]⁺. (For the heavier ytterbium metal only the fragment [Yb₂(en')₂Cl₂]⁺ was detected due to limitations in the accessible mass spectrum range.) These data imply that the complexes have a dimeric structure of the type [Ln(en')₂(μ-Cl)]₂ and contradict an earlier proposal of a monomeric structure for the Er complex also based on MS data.^[27] Verification by X-ray diffraction studies has been unsuccessful owing to the difficulty in obtaining suitable crystals of the highly soluble complexes and an unsatisfactory data solution for the one set of apparently suitable crystals (**3d**).

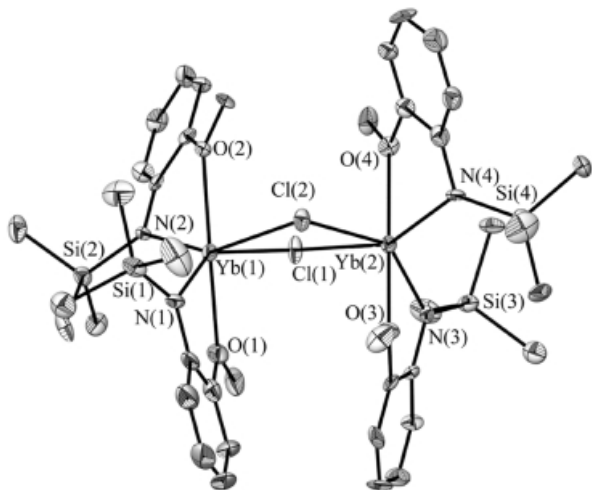


Figure 3. ORTEP view of one molecule of [Yb(L¹)₂(μ-Cl)]₂ (**4a**) drawn with 50% ellipsoids; hydrogen atoms have been omitted for clarity

The molecular structures of **4a** (Figure 3), **4b**, **4c** and **5a**·(PhMe)₂ (Figure 4) are dimeric with two lanthanoid atoms bridged by two chlorine atoms. The complexes **4a–4c** are isostructural and have the monoclinic centrosymmetric space group *P*2₁/*m* with one dimer comprising the asymmetric unit. For **5a**·(PhMe)₂ a toluene of crystallis-

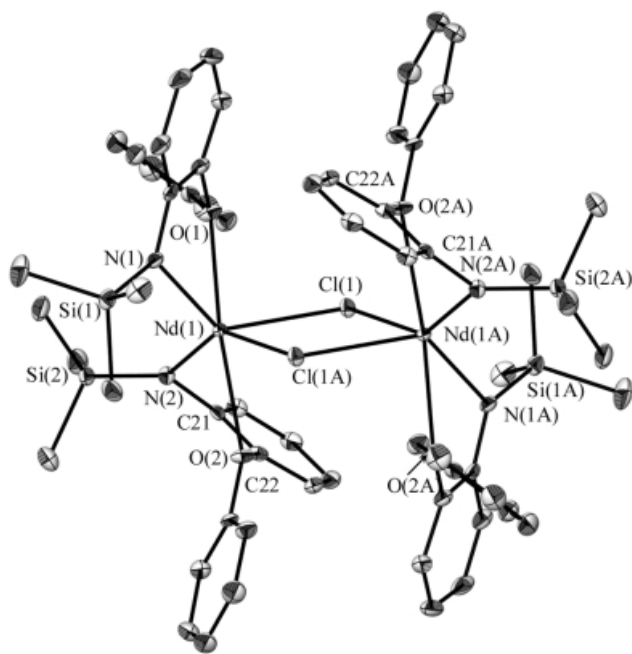


Figure 4. ORTEP view of [Nd(L²)₂(μ-Cl)]₂(PhMe)₂ (**5a**·(PhMe)₂) drawn with 50% ellipsoids; hydrogen atoms and toluene of crystallisation have been omitted for clarity

ation is present in each asymmetric unit that comprises half the dimer with a crystallographic inversion centre located in the middle of the Nd₂Cl₂ plane. Selected bond lengths and angles for **4a–4c** and **5a**·(PhMe)₂ are given in Table 3. Two chelating [L][−] (L = L¹ or L²) units are bound to each lanthanoid centre in a similar fashion completing a six-coordination environment with a very distorted octahedral geometry. Clearly, the steric demand of two L ligands and one chloride is not sufficient to saturate all coordination sites on the lanthanoid metal since dimerisation takes place. Coordination of a molecule of THF generating monomeric [Ln(L)₂Cl(THF)] may occur in THF solution prior to workup in nonpolar solvents. The chloride-bridged dimer is presumably less crowded than [Ln(L)₂Cl(THF)] with the steric coordination number^[51] for THF (1.2) larger than that for chloride (1.0). In addition, longer Ln–μ-Cl than Ln–Cl_{ter} distances also reduce crowding. These factors favour elimination of any coordinated THF on isolation.

The coordination geometry in [Ln(L)₂(μ-Cl)]₂ is similar to that of the homoleptic derivatives [Ln(L)₃] (L = L¹, L²). Two bridging chloride atoms in the former replace one equatorial L ligand of [Ln(L)₃]. The axial positions are occupied by the O(Me/Ph) group on L¹ or L² with O(1)–Ln(1)–O(2) angles close to the expected 180°. The remaining NSiMe₃ units and chloride atoms are located in mutually *cisoid* equatorial sites with the former lying above and below the equatorial plane. This arrangement presumably minimises steric repulsion between the *cis* NSiMe₃ groups as is also observed for the homoleptic complexes [Ln(L)₃] (see above). Generally the binding of the L¹ and L² ligands is similar to that in the corresponding homoleptic complexes, although there is a marginal shortening of the

Table 3. Metal environment in $[\text{Ln}(\text{L})_2(\mu\text{-Cl})_2]$ complexes

Complex	$[\text{Yb}(\text{L}^1)_2(\mu\text{-Cl})_2]$ (4a)	$[\text{Er}(\text{L}^1)_2(\mu\text{-Cl})_2]$ (4b)	$[\text{Tb}(\text{L}^1)_2(\mu\text{-Cl})_2]$ (4c)	$[\text{Nd}(\text{L}^2)_2(\mu\text{-Cl})_2(\text{PhMe})_2]$ 5a(PhMe) ₂
Bond length (Å)				
Ln(1)–N(1,2)	2.184(8), 2.190(7)	2.233(3), 2.221(3)	2.266(3), 2.265(3)	Nd(1)–N(1,2) 2.319(2), 2.299(2)
Ln(2)–N(3,4)	2.188(8), 2.202(8)	2.225(3), 2.223(3)	2.257(3), 2.257(3)	Nd(1)–O(1,2) 2.519(2), 2.567(2)
Ln(1)–O(1,2)	2.350(7), 2.370(6)	2.354(2), 2.383(2)	2.416(3), 2.437(3)	Nd(1)–Cl(1,1A) ^[a] 2.785(1), 2.856(1) ^[a]
Ln(2)–O(3,4)	2.337(7), 2.354(6)	2.353(2), 2.363(2)	2.414(3), 2.414(3)	Nd(1)–C(21) 2.911(2)
Ln(1)–Cl(1,2)	2.680(2), 2.668(3)	2.713(1), 2.683(1)	2.748(1), 2.727(1)	Nd(1)–C(22) 3.035(2)
Ln(2)–Cl(1,2)	2.678(2), 2.675(2)	2.701(1), 2.703(1)	2.740(1), 2.734(1)	
Ln(1)–Ln(2)	4.066(1)	4.1048(8)	4.1545(9)	Nd(1)–Nd(2) 4.385(5)
Angles (°)				
N(1,3)–Ln(1)–N(2,4)	113.5(3), 112.7(3)	113.80(10), 113.21(10)	116.34(11), 117.06(11)	N(1)–Nd(1)–N(2) 114.69(7)
O(1,3)–Ln(1)–O(2,4)	162.2(3), 166.6(2)	162.54(8), 168.31(7)	161.28(9), 166.85(9)	O(1)–Nd(1)–O(2) 152.65(5)
Cl(1)–Ln(X)–Cl(2) (X = 1,2)	79.55(7), 79.47(7)	79.57(3), 79.42(3)	79.38(3), 79.42(3)	Cl(1)–Nd(1)–Cl(1A) 77.96(2) ^[a]
Ln(1)–Cl(X)–Ln(2) (X = 1,2)	98.72(8), 99.12(8)	98.62(3), 99.31(3)	98.41(3), 99.05(4)	Nd(1)–Cl(1)–Nd(1A) 102.04(2) ^[a]
N(1,2)–Ln(1)–O(1,2)	71.5(3), 71.1(2)	69.83(9), 70.84(9)	68.23(11), 69.45(10)	N(1,2)–Nd(1)–O(1,2) 67.53(6), 68.47(7)
N(3,4)–Ln(2)–O(3,4)	71.8(3), 72.0(3)	70.72(9), 71.47(9)	69.01(10), 69.82(10)	
N(1,3)–Ln(1,2)–O(2,4)	124.7(3), 120.0(3)	126.23(9), 119.63(9)	129.52(10), 123.66(10)	N(1)–Nd(1)–O(2) 137.36(6)
N(1,2)–Ln(1)–Cl(1,2)	88.5(2), 91.0(2)	88.85(7), 90.89(7)	88.71(9), 89.51(8)	N(1)–Nd(1)–Cl(1, 1A) 128.17(5), 87.21(6) ^[a]
N(1,2)–Ln(1)–Cl(2,1)	144.3(2), 151.2(2)	143.13(7), 150.89(7)	141.33(9), 149.43(8)	N(2)–Nd(1)–Cl(1, 1A) 104.20(5), 145.91(5) ^[a]
N(3,4)–Ln(2)–Cl(1,2)	143.3(2), 152.3(2)	142.32(7), 151.24(7)	140.26(8), 149.06(8)	
N(3,4)–Ln(2)–Cl(2,1)	86.7(2), 93.8(2)	86.64(7), 94.36(7)	86.33(9), 92.06(8)	
O(1,2)–Ln(1)–Cl(1,2)	108.49(19), 86.81(16)	108.02(7), 86.65(6)	107.56(7), 85.10(7)	O(1)–Nd(1)–Cl(1,1A) 78.61(5), 121.30(5) ^[a]
O(2,1)–Ln(1)–Cl(1,2)	81.17(16), 80.6(2)	81.12(6), 80.64(7)	81.19(7), 80.48(8)	O(2)–Nd(1)–Cl(1,1A) 87.60(5), 77.73(5) ^[a]
O(3,4)–Ln(2)–Cl(1,2)	79.92(18), 81.31(17)	79.89(6), 80.72(6)	79.30(7), 80.48(7)	
O(3,4)–Ln(2)–Cl(2,1)	106.82(18), 91.37(17)	106.38(6), 92.58(6)	105.33(7), 90.41(7)	
N(1,2)–Ln(1)–O(2,1)	124.7(3), 96.5(3)	126.23(9), 92.29(9)	129.52(10), 98.40(11)	N(2)–Nd(1)–O(1) 91.99(7)
N(3,4)–Ln(2)–O(4,3)	120.0(3), 98.2(3)	119.63(9), 100.00(9)	123.66(10), 102.11(10)	

^[a] Symmetry transformations used to generate equivalent atoms: $-x + 2, -y + 2, -z + 1$.

Ln–N and Ln–O bond lengths consistent with the lower steric demand of two chlorides. The near planar (4a–4c) or planar [5a(PhMe)₂] Ln₂Cl₂ cores exhibit symmetrical bridging of the chlorides in the L¹ complexes, although there is a difference of 0.07 Å between the two Nd–Cl distances of 5a(PhMe)₂. The distance between the lanthanoid centres is nonbonding (Table 3) and varies in line with the ionic radii of the respective metals (Table 2).

A notable feature of the coordination of the two L² ligands to neodymium in 5a(PhMe)₂ is the noticeable tilt in one of the aromatic backbones [C(21)–C(26)]. Thus the interplanar angle to the Nd–N–O plane is 61.41(7)° which is almost double that of the other L² ligand [31.49(6)°] and of the maximum observed for the homoleptic [Ln(L²)₃] derivatives. Associated with this tilt, two of the carbon atoms [C(21) and C(22)] approach the metal centre with distances of 2.911(2) and 3.035(2) Å, respectively, which are approximately 0.25 Å shorter than the corresponding distances for the other L² ligand. The former Nd–C distances are only marginally longer than π -arene lanthanoid interactions in, for example, [Nd(η^6 -PhH)(AlCl₄)₃]^[52] [Nd–C distances of 2.93(2) to 2.94(2) Å], and are similar to or shorter than intramolecular π -arene contacts [2.964(7)–3.158(9) Å] in neodymium aryloxide complexes such as [Nd(Odpp)₃] (Odpp[−] = 2,6-diphenylphenolate).^[53] Thus, it appears that C(21) and C(22) form an intramolecular π - η^2 interaction with Nd and this bonding accounts for the tilt of the arene backbone.

For 3a–3e, a similar dimeric structural type would be expected with *cis*-amide groups, *trans*-amine substituents and bridging chloride ions per six-coordinate lanthanoid

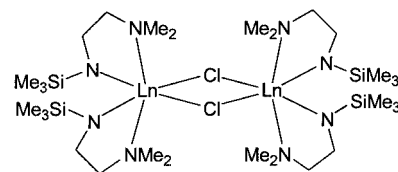


Figure 5. Postulated dimeric representation of $[\text{Ln}(\text{en})_2(\mu\text{-Cl})_2]$

centre (Figure 5), although other arrangements may also be possible.

Subtraction of the appropriate ionic radii from the Ln–Cl distances gives similar values to those of structurally characterised lanthanoid μ -chloride fragments supported by either amide or halide co-ligands (Table 2). For $[\text{Nd}(\text{L}^2)_2(\mu\text{-Cl})_2]$ one value is slightly larger than in 4a–4c complexes consistent with the greater steric crowding in the L² complex. Subtraction values for 4a–4c and 5a(PhMe)₂ are similar to $[\text{Yb}(\text{Cl})_2(\mu\text{-Cl})(\text{THF})_2]_2$ {which has an analogous donor array to $[\text{Yb}(\text{L}^1)_2(\mu\text{-Cl})_2]$ ^[47] but are longer than those from the Yb–Cl distances of $[\text{Yb}(\text{C}_5\text{H}_5)_2(\mu\text{-Cl})_2]$,^[44] consistent with the greater steric coordination number^[51] summation for $[\text{Yb}(\text{Cl})_2(\mu\text{-Cl})(\text{THF})_2]_2$ (6.42) than $[\text{Yb}(\text{C}_5\text{H}_5)_2(\mu\text{-Cl})_2]$ (6.08). The subtraction values for the Ln–Cl bonds in $[\text{Ln}(\text{L}^1)_2(\mu\text{-Cl})_2]$ are similar to those of $[\text{Sm}(\text{C}_5\text{Me}_5)_2(\mu\text{-Cl})_3]$ ^[46] (Table 2) suggesting a steric similarity between L¹ and C₅Me₅, even though the current structures are more like those of the unsubstituted cyclopentadienyl complex $[\text{Yb}(\text{C}_5\text{H}_5)_2(\mu\text{-Cl})_2]$, as the Sm(C₅Me₅)₂ groups are rotated by 90°.^[46] This may reflect both the more adaptable coordination environment of the

“edge-on” bound bidentate organoamide ligands compared with the “face-on” cyclopentadienyl ligand.

Synthesis and Crystal Structure of $[\text{Li}(\text{L}^1)(\text{OEt}_2)]_2$

The lithiation of L^1H with one equivalent of $n\text{BuLi}$ in Et_2O afforded a white precipitate of $[\text{Li}(\text{L}^1)(\text{OEt}_2)]_2$. Satisfactory elemental analyses, despite numerous attempts, could not be obtained. The values are closer to those for LiL^1 and could suggest that loss of coordinated ether occurs during the lengthy journey to the analysis laboratories. However the ^1H NMR spectrum of $[\text{Li}(\text{L}^1)(\text{OEt}_2)]_2$ established the L^1 to Et_2O ratio, and showed a single methoxy ether peak and characteristic arene backbone signals (H-3–H-6). The room temperature ^7Li NMR spectrum of $[\text{Li}(\text{L}^1)(\text{OEt}_2)]_2$ shows a single lithium environment with a narrow ($\Delta\nu_{1/2} = 14$ Hz) signal. The IR spectrum contained absorptions typical of a coordinated Et_2O molecule and of the L^1 ligand.

Crystals of $[\text{Li}(\text{L}^1)(\text{OEt}_2)]_2$ suitable for X-ray crystallography were obtained by recrystallisation of the crude material from diethyl ether. The structure of the complex $[\text{Li}(\text{L}^1)(\text{OEt}_2)]_2$ is dimeric (Figure 6). Selected geometric data are compiled in Table 4. Each four-coordinate lithium atom is surrounded by one diethyl ether, two bridging amide nitrogens [N(1) and N(1A)] and a methoxy oxygen atom in a distorted tetrahedral array. This distortion presumably

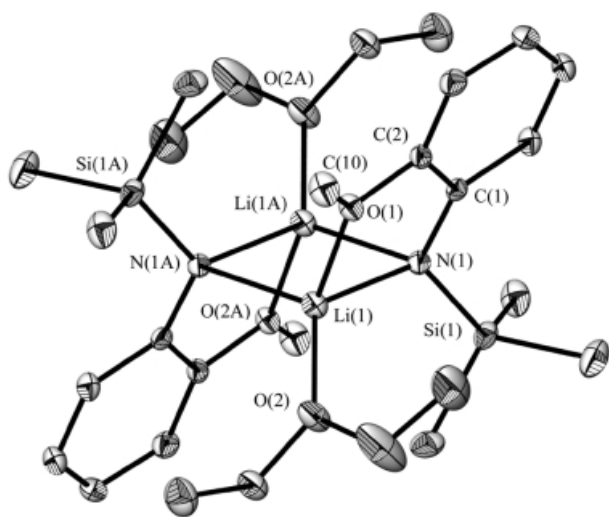


Figure 6. ORTEP view of $[\text{Li}(\text{L}^1)(\text{OEt}_2)]_2$ drawn with 50% ellipsoids; hydrogen atoms have been omitted for clarity

Table 4. Selected bond lengths (Å) and angles ($^\circ$) with estimated standard deviations in parentheses for $[\text{Li}(\text{L}^1)(\text{OEt}_2)]_2$

Li(1)–N(1)	2.028(4)	O(2)–Li(1)–O(1)	107.2(2)
Li(1)–N(1A) ^[a]	2.157(4)	O(2)–Li(1)–N(1)	124.3(2)
Li(1)–O(1)	2.000(4)	O(1)–Li(1)–N(1)	83.6(2)
Li(1)–O(2)	1.991(4)	O(2)–Li(1)–N(1A) ^[a]	120.7(2)
		O(1)–Li(1)–N(1A) ^[a]	109.4(2)
		N(1)–Li(1)–N(1A) ^[a]	104.9(2)

^[a] Symmetry transformations used to generate equivalent atoms: $-x, -y + 1, -z$.

arises from the restriction of the N–Li–O(Me) bite angle [83.6(2) $^\circ$] as well as the ligation of the bridging amide nitrogens, N(1) and N(1A), to Li(1,1A). The N(1)–Li(1)–N(1A)–Li(1A) ring is essentially planar having the bidentate L^1 ligands parallel to each other, with the arene backbone approximately perpendicular to the central (NLi)₂ plane [74.9(1) $^\circ$]. In comparison with L^1H ,^[28] binding of L^1 to lithium has little effect on the methoxy position in relation to the arene backbone plane [torsion angle: C(13)–C(12)–O(1)–C(10) 11.7(3) $^\circ$]. The structure of $[\text{Li}(\text{L}^1)(\text{OEt}_2)]_2$ can be compared with those of other sterically-crowded $[\{\text{Li}(\mu\text{-L})(\text{OEt}_2)\}_2]$ complexes [L = 8-quinolinyl-(trimethylsilyl)amide (qsta)^[54] or *N,N'*-di-*p*-tolylformamidinate (dtf)^[55]]. However, the steric requirements for L^1 must be less than that of *en'* which coordinates to lithium in an unsymmetrical dinuclear configuration in $[\text{Li}(\text{en}')_2\text{Li}(\text{OEt}_2)]$ ^[27] with one four-coordinate and one three-coordinate Li. The Li–O(1) and Li–O(2) ether distances [2.000(4) Å, 1.991(4) Å respectively] in $[\text{Li}(\text{L}^1)(\text{OEt}_2)]_2$ are similar to those in related etherates (e.g. 1.94(3) Å in four-coordinate $[\{\text{Li}(\text{qsta})(\text{OEt}_2)\}_2]$ and 1.943(6) Å in three-coordinate $[\{\text{Li}[\text{N}(\text{SiMe}_3)_2(\text{OEt}_2)]_2\}$ ^[49]). The lithium bridging is not symmetrical as shown by the significant difference in the Li(1)–N(1) and Li(1)–N(1A) bond lengths of 0.129 Å. This unsymmetrical behaviour has been observed in the related $[\{\text{Li}(\text{qsta})(\text{OEt}_2)\}_2]$ complex with bridging Li–N(amide) distances of 2.07(2) and 2.21(2) Å and is presumably due to the steric crowding by the chelating L^1 ligand. The sharp ^7Li and ^1H NMR spectra of $[\text{Li}(\text{L}^1)(\text{OEt}_2)]_2$ are consistent with observation of only one LiL^1 environment in the solid state.

Conclusions

The preparation of solvent-free lanthanoid organoamide complexes of the type $[\text{LnL}_3]$ or $[\text{Ln}(\text{L})_2(\mu\text{-Cl})_2]$ (L = L^1 , L^2 , *en'*) can be achieved through incorporation of a pendant donor on the amide ligand. For the ether-substituted L^1 and L^2 derivatives, isolation of $[\text{Ln}(\text{L})_2(\mu\text{-Cl})_2]$ is critically dependent upon the correct choice of, and size of, the ligand and the lanthanoid metal, since otherwise rearrangement to the homoleptic complex is observed. The $[\text{Ln}(\text{L})_2(\mu\text{-Cl})_2]$ (L = L^1 , L^2 , *en'*) complexes represent a new class of solvent-free heteroleptic lanthanoid(III) amides which should be capable of further functionalisation by replacement of the halide.

Experimental Section

All reactions were carried out under dry nitrogen using dry box and standard Schlenk techniques. Solvents were dried by distillation from sodium wire/benzophenone. IR data (4000–650 cm^{-1}) were recorded for Nujol mulls sandwiched between NaCl plates with a Perkin–Elmer 1600 Fourier transform infrared spectrometer. NMR spectra were obtained either on a Bruker AC200 MHz (^1H) or a Bruker AC 400 MHz spectrometer (^7Li and ^1H) as indicated. Deuterated solvents were degassed and distilled from Na/K

alloy prior to use. ^1H NMR spectra were referenced to the solvent (C_6D_6 and C_7D_8) signals; the chemical shift for the ^7Li spectrum is given relative to external 0.1 M LiCl in D_2O at room temperature. Mass spectra were recorded with a VG Trio-1 GC mass spectrometer. Each listed m/z value for metal-containing ions is the most intense peak of a cluster pattern in good agreement with the calculated pattern. Elemental analyses (C, H N) were determined by the Campbell Microanalytical Service, University of Otago, New Zealand. Lanthanoid analyses were by complexometric titration with $[\text{Na}_2\text{EDTA}]$,^[53,56] $[\text{LnCl}_3(\text{THF})_n]$,^[35] LnCl_3 ,^[57] L^1H ,^[28] L^2H ,^[28,29] $\text{en}'\text{H}$,^[27] $[\text{Li}(\text{L}^2)(\text{DME})]^{[29]}$ were each prepared according to a reported procedure. $n\text{BuLi}$ (1.6 M) (Aldrich) was used unstandardised but transferred to and stored in a Schlenk flask under nitrogen immediately on opening a new batch.

[Yb(L¹)₃] (1a). Method 1: $[\text{Li}(\text{L}^1)(\text{OEt}_2)_2]$ (0.62 g, 1.12 mmol) was added to a stirred suspension of $[\text{YbCl}_3(\text{THF})_3]$ (0.37 g, 0.75 mmol) in THF (40 mL) and the resulting mixture was stirred for 12 h. The solvent was removed under vacuum and hexane added (30 mL) giving a white precipitate. The red solution was filtered and the filtrate concentrated to 15 mL. A red crystalline product was obtained on standing for 2 h (0.41 g, 72%). IR (Nujol): $\tilde{\nu} = 1593$ vs, 1561 vs, 1485 s, 1465 m, 1321 vs, 1294 vs, 1283 s, 1245 vs, 1209 s, 1159 w, 1059 w, 1051 s, 1012 s, 1000 vs, 913 br. s, 843 br vs, 822 s, 787 m, 770 s, 743 s, 681 s, 629 s, 598 s cm^{-1} . Vis/near IR (DME): λ_{max} (ϵ) = 431 (185), 874 (9), 911 (14), 945 (6), 978 (35) nm ($\text{dm}^3 \text{mol}^{-1}$). $\text{C}_{30}\text{H}_{48}\text{N}_3\text{O}_3\text{Si}_3\text{Yb}$ (756.23): calcd. C 47.66, H 6.40, N 5.56; found C 47.88, H 6.44, N 5.63.

Method 2 [2:1 Li to Ln mol ratio (in situ): $n\text{BuLi}$ was slowly added (2.31 mL, 3.70 mmol) to a stirred solution of L^1H (0.71 g, 3.60 mmol) in THF (40 mL) at 0 °C and the resulting solution was warmed to room temperature over ca. 1 h. $[\text{YbCl}_3(\text{THF})_2]$ (0.76 g, 1.80 mmol) was added to the resulting solution and the reaction mixture rapidly stirred for 12 h. The solvent was removed in vacuo, and hexane (30 mL) was added affording a white precipitate. The red solution was filtered and the filtrate volume reduced to ca. 2 mL under vacuum. Red crystals of $[\text{Yb}(\text{L}^1)_3]$ (**1a**) were deposited on standing overnight. The infrared spectrum was identical to that of **1a** obtained from **Method 1**.

[Er(L¹)₃] (1b): $n\text{BuLi}$ (2.30 mL, 3.70 mmol) was added to a stirred solution of compound L^1H (0.72 g, 3.70 mmol) in THF (40 mL) at 0 °C, and the resulting solution was warmed to room temperature over ca. 1 h. $[\text{ErCl}_3(\text{THF})_{3.5}]$ (0.63 g, 1.20 mmol) was then added and the reaction mixture stirred for 15 h. The solvent was then removed under vacuum and hexane (30 mL) was added giving a white precipitate. The light pink solution was filtered and the filtrate volume reduced to 10 mL under vacuum. The light pink crystals deposited on standing for 12 h (0.43 g, 48%). IR (Nujol): $\tilde{\nu} = 1593$ vs, 1561 vs, 1485 s, 1464 m, 1321 vs, 1284 vs, 1240 s, 1209 s, 1156 vs, 1117 vs, 1058 w, 1051 s, 1011 s, 1000 vs, 911 br. s, 841 br vs, 784 s, 768 s, 735 s, 681 s, 627 s, 597 s cm^{-1} . MS: m/z (%) = 646 (<1) $[\text{Er}(\text{L}^1)_2\text{NC}_6\text{H}_4]^+$, 556 (<1) $[\text{Er}(\text{L}^1)_2]^+$, 480 (<1) $[\text{Er}(\text{L}^1)(\text{C}_6\text{H}_4\text{NSi})]^+$, 195 (35) $[(\text{L}^1\text{H})]^+$, 180 (20) $[(\text{L}^1\text{H}) - \text{Me}]^+$, 165 (100) $[(\text{L}^1\text{H}) - 2\text{Me}]^+$, 150 (35) $[(\text{L}^1\text{H}) - 3\text{Me}]^+$, 135 (20) $[\text{C}_6\text{H}_5\text{ONSi}]^+$, 73 (20) $[\text{SiMe}_3]^+$, 58 (10) $[\text{SiMe}_2]^+$. $\text{C}_{30}\text{H}_{48}\text{ErN}_3\text{O}_3\text{Si}_3$ (748.22): calcd. C 48.03, H 6.45, N 5.60; found C 48.16, H 6.70, N 5.73.

[Sm(L¹)₃] (1c): A similar preparation method to that used for compound **1b** gave yellow crystals of **1c** (0.36 g, 41%). IR (Nujol): $\tilde{\nu} = 1585$ vs, 1559 vs, 1481 s, 1307 vs, 1279 vs, 1237 s, 1211 s, 1173 vs, 1117 vs, 1076 vs, 1058 w, 1050 vs, 1030 vs, 937 s, 919 s, 842 s, 825 s, 772 vs, 741 vs, 735 s, 662 vs, 616 s, 597 s cm^{-1} . MS: m/z (%) =

734 (<1) $[\text{Sm}(\text{L}^1)_3]^+$, 630 (<1) $[\text{Sm}(\text{L}^1)_2\text{NC}_6\text{H}_4]^+$, 540 (<1) $[\text{Sm}(\text{L}^1)_2]^+$, 464 (<1) $[\text{Sm}(\text{L}^1)(\text{C}_6\text{H}_4\text{NSi})]^+$, 195 (35) $[(\text{L}^1\text{H})]^+$, 180 (20) $[(\text{L}^1\text{H}) - \text{Me}]^+$, 165 (100) $[(\text{L}^1\text{H}) - 2\text{Me}]^+$, 150 (35) $[(\text{L}^1\text{H}) - 3\text{Me}]^+$, 135 (20) $[\text{C}_6\text{H}_5\text{ONSi}]^+$, 73 (20) $[\text{SiMe}_3]^+$, 58 (10) $[\text{SiMe}_2]^+$. $\text{C}_{30}\text{H}_{48}\text{N}_3\text{O}_3\text{Si}_3\text{Sm}$ (734.21): calcd. C 49.13, H 6.60, N 5.73; found C 48.55, H 6.67, N 5.67.

[Pr(L¹)₃] (1d): A similar preparation method to that used for compound **1b** gave green crystals of **1d** (0.49 g, 57%). IR (Nujol): $\tilde{\nu} = 1590$ vs, 1561 vs, 1484 s, 1449 s, 1320 vs, 1285 vs, 1246 br. s, 1210 s, 1164 vs, 1117 vs, 1058 w, 1050 s, 1011 s, 1002 vs, 915 br. s, 841 br. s, 768 s, 743 s, 674 s, 625 s, 597 s cm^{-1} . $\text{C}_{30}\text{H}_{48}\text{N}_3\text{O}_3\text{PrSi}_3$ (723.21): calcd. C 49.78, H 6.68, N 5.80; found C 49.56, H 6.71, N 5.97.

[Nd(L¹)₃] (1e). Method 1: A similar preparation method to that used for compound **1b** gave blue crystals of **1e** (0.57 g, 65%). IR (Nujol): $\tilde{\nu} = 1590$ vs, 1560 m, 1484 s, 1319 vs, 1285 vs, 1246 m, 1209 s, 1163 s, 1117 vs, 1058 w, 1050 s, 1011 s, 1002 vs, 914 br. s, 841 br vs, 767 s, 743 vs, 675 m, 625 s, 597 s cm^{-1} . MS: m/z (%) = 726 (10) $[\text{Nd}(\text{L}^1)_3]^+$, 622 (5) $[\text{Nd}(\text{L}^1)_2\text{C}_6\text{H}_4\text{N}]^+$, 532 (30) $[\text{Nd}(\text{L}^1)_2]^+$, 305 (5) $[\text{Nd}(\text{L}^1) - \text{OMe}]^+$, 195 (40) $[(\text{L}^1\text{H})]^+$, 180 (15) $[(\text{L}^1\text{H}) - \text{Me}]^+$, 165 (70) $[(\text{L}^1\text{H}) - 2\text{Me}]^+$, 150 (30) $[(\text{L}^1\text{H}) - 3\text{Me}]$, 135 (25) $[\text{C}_6\text{H}_5\text{ONSi}]^+$, 73 (100) $[\text{SiMe}_3]^+$, 58 (35) $[\text{SiMe}_2]^+$. ^1H NMR (300 MHz, C_6D_6 , 298 K): $\delta = -16.98$ (br. s, 9 H, OMe), -4.20 (br. s, 27 H, SiMe₃), 1.14 (s, 3 H, H-4 or H-5), 7.88 (s, 3 H, H-4 or H-5), 14.18 (s, 3 H, H-3 or H-6), 23.60 (s, 3 H, H-3 or H-6). $\text{C}_{30}\text{H}_{48}\text{N}_3\text{NdO}_3\text{Si}_3$ (724.21): calcd. C 49.55, H 6.65, N 5.78; found C 49.85, H 6.81, N 5.73.

Method 2 [using 1:2 Ln to L¹ mol ratio (in situ): $n\text{BuLi}$ (2.31 mL, 3.70 mmol) was slowly added to a stirred solution of compound L^1H (0.71 g, 3.60 mmol) in THF (40 mL) at 0 °C and the resulting solution was warmed to room temperature over ca. 1 h. $[\text{NdCl}_3(\text{THF})_2]$ (0.71 g, 1.80 mmol) was added to the resulting solution, and the reaction mixture was stirred rapidly for 12 h. The solvent was removed in vacuo, and hexane (30 mL) was added affording a white precipitate. The blue solution was filtered and the filtrate volume was reduced to ca. 2 mL under vacuum. Blue crystals deposited on standing overnight. The infrared spectrum was similar to that of **1e** (**Method 1**). Unit Cell data [$\text{C}_{30}\text{H}_{48}\text{N}_3\text{NdO}_3\text{Si}_3$, $M = 724.2$, monoclinic, $a = 10.121(1)$, $b = 18.876(1)$, $c = 18.814(1)$ Å; $\alpha = 90^\circ$, $\beta = 104.37(1)^\circ$, $\gamma = 90^\circ$; $V = 3500.2$ Å³, $T \approx 123$ K] were in agreement with those of $[\text{Nd}(\text{L}^1)_3]$ from **Method 1** (Table 5).

Method 3 [using 1:2 Ln to Li (isolated) ratio]: $[\text{NdCl}_3(\text{THF})_2]$ (0.30 g, 0.75 mmol) and $[\text{Li}(\text{L}^1)(\text{OEt}_2)_2]$ (0.42 g, 0.75 mmol) were stirred together in THF (40 mL). After 12 h, the pale yellow solution was evaporated to dryness under reduced pressure and hexane added. The resulting white solid was filtered and the filtrate evaporated to dryness under vacuum affording a blue crystalline material (0.20 g, 55%). Infrared and ^1H NMR spectra were identical to those of **1e** (**Method 1**).

[Yb(L²)₃](PhMe) [2a·(PhMe)]: $n\text{BuLi}$ (1.88 mL, 3.00 mmol) was added to a stirred solution of L^2H (0.77 g, 3.00 mmol) in THF (40 mL) at 0 °C, and the resulting solution was warmed to room temperature over ca. 1 h. $[\text{YbCl}_3(\text{THF})_2]$ (0.42 g, 1.0 mmol) was then added and the reaction mixture was stirred for 12 h. The solvent was then removed under vacuum and toluene (30 mL) was added giving a white precipitate. The red solution was filtered at -78 °C and the filtrate volume reduced to 25 mL under vacuum. Red crystals of good X-ray quality were deposited on standing overnight (0.70 g, 68%). IR (Nujol): $\tilde{\nu} = 1593$ vs, 1558 m, 1480 s, 1278 vs, 1241 vs, 1186 vs, 1152 vs, 1097 s, 1072 w, 1051 s, 1020 m, 1005 w, 906 s, 858 sh w, 840 s, 824 s, 802 s, 778 m, 728 s, 692 vs, 626 w,

Table 5. Crystallographic and refinement parameters for [Ln(L)₃] complexes

Compound	[Nd(L ¹) ₃] 1e	[Yb(L ²) ₃](PhMe) 2a ·(PhMe)	[Nd(L ²) ₃] 2d	[La(L ²) ₃] 2e
Empirical formula	C ₃₀ H ₄₈ N ₃ NdO ₃ Si ₃	C ₅₂ H ₆₂ N ₃ O ₃ Si ₃ Yb	C ₄₅ H ₅₄ N ₃ NdO ₃ Si ₃	C ₄₅ H ₅₄ LaN ₃ O ₃ Si ₃
Molecular Weight	727.22	1034.36	913.42	908.09
Crystal system	monoclinic	triclinic	monoclinic	monoclinic
Space Group	<i>P2₁/c</i>	<i>P1bar</i>	<i>P2₁/n</i>	<i>P2₁/n</i>
Crystal size [mm]	0.25 × 0.20 × 0.13	0.25 × 0.18 × 0.10	0.35 × 0.28 × 0.27	0.30 × 0.25 × 0.20
<i>a</i> [Å]	10.1207(3)	13.4071(3)	16.1450(2)	16.2330(1)
<i>b</i> [Å]	18.9788(6)	13.4511(3)	15.4738(2)	15.4788(1)
<i>c</i> [Å]	18.8243(2)	14.7899(2)	18.0246(2)	18.0579(2)
α [deg]	90	100.240(1)	90	90
β [deg]	104.376(1)	92.274(1)	103.032(1)	103.313(1)
γ [deg]	90	110.243(1)	90	90
<i>V</i> [Å ³]	3502.5(12)	2447.8(9)	4387.0(15)	4415.4(15)
<i>Z</i>	4	2	4	4
<i>d</i> _{calcd} (g cm ⁻³)	1.379	1.403	1.383	1.366
<i>F</i> (000)	1500	1062	1884	1872
μ (Mo- <i>K</i> α) (mm ⁻¹)	1.617	2.028	1.307	1.090
$2\theta_{\max}$ (°)	56.6	61.0	56.6	56.6
<i>N</i> , <i>N</i> _o	8539, 5881	13093, 10634	10849, 9244	10885, 8914
<i>Goof</i>	1.033	1.038	1.025	1.021
<i>R</i> , <i>R</i> _w (observed data)	0.0343, 0.0612	0.0394, 0.0744	0.0271, 0.0588	0.0277, 0.0607
<i>R</i> , <i>R</i> _w (all data)	0.0673, 0.0693	0.0601, 0.0838	0.0378, 0.0629	0.0417, 0.0645

591 s, 568 w cm⁻¹. MS: *m/z* (%) = 942 (<1) [Yb(L²)₃]⁺, 849 (<1) [Yb(L²)₃(C₆H₄NSiMe₃)⁺, 776 (16) [Yb(L²)₂(C₆H₄N)]⁺, 686 (35) [Yb(L²)₂]⁺, 671 (15) [Yb(L²)₂ - Me]⁺, 609 (18) [Yb(L²)(OC₆H₄NSiMe₃)⁺, 593 (3) [Yb(L²)(C₆H₄NSiMe₃)⁺, 523 (4) [Yb(L²)OC₆H₅]⁺, 430 (30) [Yb(L²)]⁺, 415 (35) [Yb(L²) - Me]⁺, 400 (7) [Yb(L²) - 2Me]⁺, 353 (3) [Yb(OC₆H₄NSiMe₃)⁺, 337 (5) [Yb(C₆H₄NSiMe₃)⁺, 257 (20) [(L²H)]⁺, 242 (16) [(L²H) - Me]⁺, 226 (10) [(L²) - 2Me]⁺, 165 (50) [OC₆H₄NHSiMe₂]⁺, 150 (15) [C₆H₄ONHSiMe]⁺, 73 (100) [SiMe₃]⁺. C₅₂H₆₂N₃O₃Si₃Yb (1034.36): calcd. C 60.38, H 6.04, N 4.06; found C 59.69, H 6.42, N 4.35.

[Yb(L²)₃](C₅H₉Me) [2a·(C₅H₉Me)]. Method 1 (using a 1:2 Ln:Li ratio): THF (40 mL) was added to the solids [Li(L²)(DME)] (0.53 g, 1.50 mmol) and [YbCl₃(THF)₂] (0.32 g, 0.75 mmol) and the resulting mixture was stirring for 12 h. The solvent was then removed under vacuum and toluene (25 mL) added giving a white precipitate. The red solution was filtered at -78 °C and the filtrate volume reduced to 20 mL under vacuum. Red crystals of [Yb(L²)₃](C₅H₉Me) (suitable for X-ray analysis) deposited on standing overnight (0.15 g, 24% [based on L²]). IR (Nujol): $\tilde{\nu}$ = 1593 vs, 1560 m, 1480 sh w, 1307 w, 1280 s, 1242 s, 1152 s, 1185 s, 1098 s, 1072 m, 1052 s, 1020 m, 1004 w, 908 s, 858 sh w, 840 s, 824 s, 802 s, 780 m, 726 s, 691 s, 618 s cm⁻¹. MS: *m/z* (%) = 776 (<1) [Yb(L²)₂(C₆H₄N)]⁺, 686 (4) [Yb(L²)₂]⁺, 507 (4) [Yb(L²)(OC₆H₅)]⁺, 430 (10) [Yb(L²)]⁺, 415 (10) [Yb(L²) - Me]⁺, 353 (10) [Yb(OC₆H₄NSiMe₃)⁺, 337 (10) [Yb(C₆H₄NSiMe₃)⁺, 257 (45) [(L²H)]⁺, 242 (40) [(L²) - Me]⁺, 226 (5) [(L²) - 2Me]⁺, 165 (100) [OC₆H₄NSiMe₂]⁺, 150 (35) [C₆H₄ONHSiMe]⁺, 73 (50) [SiMe₃]⁺. C₅₁H₆₆N₃O₃Si₃Yb (solvate) (1026.37): calcd. C 59.68, H 6.48, N 4.09. C₄₅H₅₄N₃O₃Si₃Yb ([Yb(L²)₃]) (942.27): calcd. C 57.36, H 5.78, N 4.46; found C 57.47, H 6.01, N 4.22.

Method 2 [2:1 Li to Ln mol ratio (in situ)]: *n*BuLi (1.65 mL, 2.60 mmol) was slowly added to a stirred solution of compound L²H (0.64 g, 2.50 mmol) in THF (40 mL) at 0 °C and the resulting solution was warmed to room temperature over ca. 1 h. [YbCl₃(THF)₃] (0.66 g, 1.25 mmol) was added to the resulting solution, and the reaction mixture stirred rapidly for 12 h. The solv-

ent was removed in vacuo, and toluene (20 mL) added affording a white precipitate. The red solution was filtered and the filtrate volume reduced to ca. 2 mL under vacuum. Hexane (15 mL) was added to the oily residue resulting in an immediate precipitation of LiCl and a red solution. Red crystals deposited on standing and were dried at room temperature under vacuum. The infrared spectrum was similar to that of 2a·(C₅H₉Me) above.

[Y(L²)₃](C₅H₉Me) [2b·(C₅H₉Me)]: A similar procedure to that used for compound 2a·(PhMe) gave colourless crystals of the title complex (0.61 g, 71%). IR (Nujol): $\tilde{\nu}$ = 1592 vs, 1582 s, 1557 m, 1489 s, 1278 vs, 1239 vs, 1210 s, 1170 s, 1152 vs, 1099 vs, 1071 m, 1049 s, 1020 m, 1004 w, 911 br. s, 860 w, 824 s, 776 s, 735 vs, 692 vs, 675 w, 625 w, 592 s, 560 w cm⁻¹. MS: *m/z* (%) = 857 (<1) [Y(L²)₃]⁺, 601 (20) [Y(L²)₂]⁺, 524 (5) [Y(L²)(OC₆H₄NSiMe₃)⁺, 438 (5) [Y(L²)(OC₆H₅)]⁺, 330 (5) [Y(L²) - Me]⁺, 257 (40) [(L²H)]⁺, 242 (20) [(L²H) - Me]⁺, 164 (60) [OC₆H₄NSiMe₂]⁺, 149 (25) [C₆H₄ONHSiMe]⁺, 73 (100) [SiMe₃]⁺. ¹H NMR (300 MHz, C₆D₆, 298 K): δ = 0.43 (s, 27 H, SiMe₃), 0.89–1.45 (complex m, 6 H, C₅H₉Me), 5.97–6.15 (dd, ³*J* = 7.1, ⁴*J* = 1.2 Hz, 3 H, H-6), 6.20–6.30 (bd, ³*J* = 6.9, ⁴*J* = 1.5 Hz, 3 H, H-5), 6.40–6.97 (br. m, 21 H, H-3, H-4, H-2'-6'). C₅₁H₆₆N₃O₃Si₃Y (solvate) (941.35): calcd. C 65.01, H 7.06, N 4.46. C₄₅H₅₄N₃O₃Si₃Y ([Y(L²)₃]) (857.25): calcd. C 62.99, H 6.34, N 4.90; found C 65.70, H 7.49, N 4.46.

[Sm(L²)₃](PhMe) (2c): A similar preparation method to that used for compound 2a·(PhMe) (Method 1) gave yellow crystals of the title complex (0.56 g, 56%). IR (Nujol): $\tilde{\nu}$ = 1591 vs, 1557 w, 1480 s, 1283 vs, 1248 vs, 1186 vs, 1155 vs, 1102 vs, 1071 w, 1053 s, 1021 w, 1005 w, 915 s, 826 s, 802 vs, 774 s, 727 vs, 694 vs, 676 w, 622 s, 593 s cm⁻¹. MS: *m/z* (%) = 922 (<1%) [Sm(L²)₃]⁺ 827 (<1), [Sm(L²)₂(C₆H₄NSiMe₃)⁺, 757 (<1) [Sm(L²)₂(OC₆H₅)]⁺, 664 (10) [Sm(L²)₂]⁺, 587 (<1) [Sm(L²)(OC₆H₄NSiMe₃)⁺, 408 (3) [Sm(L²)]⁺, 392 (3) [Sm(L²) - MeH]⁺, 331 (4) [Sm(OC₆H₄NSiMe₃)⁺, 315 (5) [Sm(C₆H₄NSiMe₃)⁺, 257 (100) [(L²H)]⁺, 242 (100) [(L²H) - Me]⁺, 226 (20) [(L²) - 2Me]⁺, 165 (100) [OC₆H₄NHSiMe₂]⁺, 150 (40) [C₆H₄ONHSiMe]⁺, 73 (70) [SiMe₃]⁺. ¹H NMR (300 MHz, C₆D₆, 298 K): δ = -1.63 (s, 27 H,

SiMe₃), 2.10 (s, 3 H, PhMe), 4.26 (br. s, 6 H, H-2',H-6'), 5.31–5.45 (br. s, 6 H, H-3', H-5'), 5.49–5.60 (br. s, 3 H, H-4'), 6.30–6.50 (d, ³J = 7.5 Hz, 3 H, H-3 or H-6), 6.90–7.10 (m, 5 H, PhMe), 7.40–7.46 (t, ³J = 7.5 Hz, 3 H, H-4 or H-5), 8.28–8.31 (t, ³J = 7.4 Hz, 3 H, H-4 or H-5), 10.67–10.70 (d, ³J = 8.0 Hz, 3 H, H-3 or H-6). C₅₂H₆₂N₃O₃Si₃Sm (1012.33): calcd. C 61.73, H 6.18, N 4.15; found C 62.83, H 6.74, N 4.22.

[Nd(L²)₃](PhMe)₂ [2d·(PhMe)₂]. Method 1: A similar preparation method to that used for compound **2a**·(PhMe) gave blue crystals of the title complex (0.68 g, 62%). IR (Nujol): $\tilde{\nu}$ = 1591 vs, 1557 w, 1481 s, 1337 vs, 1285 vs, 1249 vs, 1187 vs, 1155 vs, 1103 vs, 1070 w, 1052 s, 1020 w, 1005 w, 916 vs, 826 s, 802 s, 773 s, 728 vs, 694 vs, 676 w cm⁻¹. ¹H NMR (300 MHz, C₆D₆, 298 K): δ = -8.05 (br. s, 6 H, H-2',H-6'), -1.22 (br. s, 27 H, SiMe₃), 0.48 (br. s, 6 H, H-3',H-5'), 0.90 (s, 3 H, H-4 or H-5), 1.20 (br. s, 3 H, H-4'), 2.11 (s, 6 H, PhMe), 6.97–7.14 (m, 13 H, H-4 or H-5 and PhMe), 13.90 (br. s, 3 H, H-3 or H-6), 23.28 (br. s, 3 H, H-3 or H-6). C₅₉H₇₀N₃NdO₃Si₃ (1094.38): calcd. C 64.56, H 6.43, N 3.83; found C 64.48, H 6.54, N 4.13. Recrystallisation of [Nd(L²)₃](PhMe)₂ from hexane afforded crystals of solvent free [Nd(L²)₃] (**2d**) used for X-ray crystallography.

Method 2 [2:1 Li to Ln mol ratio (in situ)]: nBuLi (1.65 mL, 2.60 mmol) was slowly added to a stirred solution of compound L²H (0.64 g, 2.50 mmol) in THF (40 mL) at 0 °C and the resulting solution was warmed to room temperature over ca. 1 h. [NdCl₃(THF)₂] (0.49 g, 1.25 mmol) was added to the resulting solution, and the reaction mixture was rapidly stirred for 12 h. The solvent was removed in vacuo, and hexane (30 mL) added affording a white precipitate. The blue solution was filtered and the filtrate volume reduced to ca. 15 mL under vacuum. Blue crystals of [Nd(L²)₃] (**2d**) deposited on standing. (Infrared identification) Unit Cell data [C₄₅H₅₄N₃NdO₃Si₃, *M* = 910.3, monoclinic, *a* = 16.154(1), *b* = 15.459(1), *c* = 17.992(1) Å; *a* = 90°, *β* = 103.0(1)°, *γ* = 90°; *V* = 4378.1 Å³, *T* ≈ 123 K] were in agreement with those obtained for crystals from **Method 1** (Table 5).

[La(L²)₃](PhMe) (2e·(PhMe)). Method 1: A similar preparation method to that used for compound **2a**·(PhMe) gave yellow crystals of the title complex (0.35 g, 35%). IR (Nujol): $\tilde{\nu}$ = 1589 vs, 1557 m, 1480 s, 1287vs, 1249 vs, 1188 vs, 1155 vs, 1103 vs, 1070 w, 1050 s, 1020 m, 1004 w, 919 s, 858 w, 824 m, 803 vs, 770 vs, 694 vs, 675 w, 618 s, 592 s, 562 w cm⁻¹. MS: *m/z* (%) = 651 (3) [La(L²)₂]⁺, 395 (<1) [La(L²)₃]⁺, 257 (70) [(L²H)]⁺, 242 (65) [(L²H) - Me]⁺, 226 (15) [(L²) - 2Me]⁺, 165 (100) [OC₆H₄NHSiMe₂]⁺, 150 (40) [C₆H₄ONHSiMe]⁺, 135 (30) [C₆H₄OSiNH]⁺, 73 (50) [SiMe₃]⁺. ¹H NMR (300 MHz, C₆D₆, 298 K): δ = 0.36 (s, 27 H, SiMe₃), 2.10 (s, 3 H, PhMe), 6.11 (dd, ³J = 8.1, ⁴J = 1.4 Hz, 3 H, H-6), 6.28 (td, ³J = 7.2, ⁴J = 1.3 Hz, 3 H, H-5), 6.74–6.90 (m, 21 H, H-3, H-4, H-2'-6'), 6.97–7.13 (m, 5 H, PhMe). C₅₂H₆₂LaN₃O₃Si₃ (999.32): calcd. C 62.44, H 6.25, N 4.20; found C 62.27, H 6.35, N 4.32. **Method 2 [La(L²)₃] (2e) (using a 1:2 Ln to Li ratio):** LaCl₃ (0.18 g, 0.75 mmol) and [Li(L²)(DME)] (0.53 g, 1.50 mmol) were stirred together in THF (40 mL). After 12 h, the pale yellow solution was evaporated to dryness under reduced pressure and toluene was added. The resulting white solid was filtered, the filtrate was evaporated to dryness and Et₂O was added (20 mL). The solution was concentrated to ca. 10 mL and on standing for two days colourless crystals of **2e** (suitable for an X-ray crystallographic study) were deposited (0.35 g, 77%). IR (Nujol): $\tilde{\nu}$ = 1590 vs, 1557 m, 1480 s, 1444 s, 1288 vs, 1251 vs, 1189 vs, 1155 vs, 1102 vs, 1072 w, 1052 s, 1020 m, 1004 w, 964 w, 917 s, 858 w, 826 m, 801 s, 771 s, 735 s, 722 s, 695 s, 674 w, 632 w, 622 s, 594 s, 559 w cm⁻¹. ¹H NMR (300 MHz, C₆D₆, 298 K): δ = 0.35 (s, 27 H, SiMe₃), 6.10

(dd, ³J = 7.6, ⁴J = 1.2 Hz, 3 H, H-6), 6.26 (td, ³J = 7.5, ⁴J = 1.6 Hz, 3 H, H-5), 6.72–6.90 (m, 21 H, H-3,H-4, H-2'-6').

Method 3 [2:1 Li to Ln ratio (in situ)]: nBuLi (1.65 mL, 2.60 mmol) was slowly added to a stirred solution of compound L³H (0.64 g, 2.50 mmol) in THF (40 mL) at 0 °C and the resulting solution was warmed to room temperature over ca. 1 h. [LaCl₃(THF)₂] (0.49 g, 1.25 mmol) was added to the resulting solution, and the reaction mixture stirred rapidly for 12 h. The solvent was removed in vacuo, and hexane (30 mL) added affording a white precipitate. The pale yellow solution was filtered and the filtrate volume reduced to ca. 15 mL under vacuum. Light yellow crystals were deposited on standing. The infrared spectrum was identical with that of [La(L²)₃] (**2e** (Method 2)).

[Yb(en')₂(μ-Cl)₂] (3a): nBuLi (3.75 mL, 6.00 mmol) was slowly added to a stirred solution of en'H (0.88 g, 1.00 mL, 5.50 mmol) in THF (50 mL) at 0 °C and the resulting solution was warmed to room temperature over ca. 1 h. [YbCl₃(THF)₃] (1.36 g, 2.75 mmol) was added to this solution, and the reaction mixture was rapidly stirred for 12 h. The solvent was removed in vacuo, and hexane added affording a white precipitate. The orange solution was filtered and the filtrate volume reduced to ca. 2 mL under vacuum. Orange crystals deposited on standing overnight (0.79 g, 55%). IR (Nujol): $\tilde{\nu}$ = 1401 w, 1351 m, 1270 w, 1258 m, 1238 m, 1176 w, 1160 w, 1105 m, 1091 m, 1078 m, 1031 w, 1010 s, 952 s, 925 s, 858 s, 832 m, 778 w, 740 m, 679 w, 665 w cm⁻¹. MS: *m/z* (%) = 736 (<1) [M(dimer) - (2 L)]⁺, 701 (<1) [Yb₂(L₂)Cl]⁺, 527 (2) [Yb(L₂)Cl]⁺, 333 (50) [Yb(L)]⁺, 73 (45) [SiMe₃]⁺, 58 (100) [SiMe₂]⁺. C₂₈H₇₆Cl₂N₈Si₄Yb₂ (1054.32): calcd. C 31.90, H 7.27, N 10.66, Yb 32.83; found C 31.35, H 7.28, N 9.60, Yb 33.18.

[Er(en')₂(μ-Cl)₂] (3b): A similar preparation method to that used for compound **3a** gave pink crystals of **3b** (0.76 g, 53%). IR in satisfactory agreement with that reported for an analytically pure sample.^[27] MS: *m/z* (%) = 883 (<1) [M(dimer) - (L)]⁺, 724 (1) [M(dimer) - (2 L)]⁺, 521 (1) [Er(L₂)Cl]⁺, 325 (25) [Er(L)]⁺, 73 (35) [SiMe₃]⁺, 58 (100) [SiMe₂]⁺.

[Sm(en')₂(μ-Cl)₂] (3c): A similar procedure to that used for compound **3a** gave yellow crystals of **3c** (0.58 g, 42%). IR (Nujol): $\tilde{\nu}$ = 1401 w, 1349 m, 1310 w, 1258 m, 1246 s, 1195 w, 1169 w, 1156 sh w, 1103m, 1087 m, 1079 m, 1035 w, 1020 s, 953 m, 924 s, 859 s, 828 br. s, 779 sh m, 735 m, 676 w, 662 m, 619 w, 554 w cm⁻¹. MS: *m/z* (%) = 689 (<1) [M(dimer) - (2 L)]⁺, 507 (1) [Sm(L₂)Cl]⁺, 348 (20) [Sm(L)Cl]⁺, 311 (15) [Sm(L)]⁺, 281 (25) [Sm(L) - 2Me]⁺, 73 (50) [SiMe₃]⁺, 58 (100) [SiMe₂]⁺.

[Nd(en')₂(μ-Cl)₂] (3d): A similar procedure to that used for compound **3a** gave blue crystals of **3d** (0.70 g, 51%). IR (Nujol): $\tilde{\nu}$ = 1348 m, 1259 m, 1246 s, 1168 w, 1104 m, 1079 m, 1154 m, 1036 w, 1020 s, 952 w, 938 s, 924 s, 851 s, 827 br. s, 780 sh m, 734 m, 676 w, 662 m, 554 w cm⁻¹. MS: *m/z* (%) = 835 (<1) [{}¹⁴⁴Nd(L₂)(μ-Cl)₂ - (L)]⁺, 676 (<1) [{}¹⁴⁴Nd(L₂(μ-Cl)₂ - (2 L)]⁺, 482 (1) [{}¹⁴⁴Nd₂(L)Cl]⁺, 338 (50) [{}¹⁴⁴Nd(L)Cl]⁺, 73 (45) [SiMe₃]⁺, 58 (100) [SiMe₂]⁺. C₂₈H₇₆Cl₂N₈Nd₂Si₄ (990.28): calcd. Nd 28.94; found Nd 29.15.

[La(en')₂(μ-Cl)₂] (3e): A similar preparation to that for compound **3a** gave colourless crystals of **3e** (0.63 g, 46%). IR (Nujol): $\tilde{\nu}$ = 1439 w, 1348 w, 1314 w, 1239 br. s, 1160 s, 1121 s, 1092 s, 1077 w, 1037 w, 1021 w, 998 m, 962 m, 923 m, 848 s, 830 br. s, 748 w, 725 m, 694 m, 664 w, 541 w cm⁻¹. MS: *m/z* (%) = 825 (5) [M(dimer) - (L)]⁺, 457 (30) [La(L₂)₂]⁺, 333 (80) [La(L)Cl]⁺, 73 (20) [SiMe₃]⁺, 58 (100) [SiMe₂]⁺. C₂₈H₇₆Cl₂La₂N₈Si₄ (984.28): calcd. La 28.17; found La 28.02.

[Yb(L¹)₂(μ-Cl)]₂ (4a): [Li(L¹)(OEt₂)₂] (0.76 g, 1.37 mmol) was added to a stirred suspension of [YbCl₃(THF)₃] (0.68 g, 1.37 mmol) in THF (40 mL). The solution was stirred for 15 h, the solvent was removed under vacuum and hexane (30 mL) was added. After heating the stirred solution for 2 h, the warm mixture was filtered and on cooling to room temperature the filtrate afforded red crystals (suitable for X-ray analysis) of the title complex (0.51 g, 63%). IR (Nujol): $\tilde{\nu}$ = 1594 s, 1563 w, 1318 w, 1290 s, 1277 s, 1242 vs, 1210 m, 1158 s, 1117 vs, 1051 m, 1002 s, 917 s, 844 vs, 826 s, 792 w, 768 m, 730 vs, 679 m, 627 w, 597 w cm⁻¹. Vis/near IR (DME): λ_{max} (ε) = 457 (156), 935 (4), 982 (18), 985 (17) nm (dm³ mol⁻¹). C₄₀H₆₄Cl₂N₄O₄Si₄Yb₂ (1194.30): calcd. C 40.23, H 5.40, N 4.69; found C 39.15, H 5.57, N 4.72.

[Er(L¹)₂(μ-Cl)]₂ (4b): Addition of [Li(L¹)(OEt₂)₂] (0.55 g, 1.00 mmol) to a suspension of [ErCl₃(THF)₂] (0.42 g, 1.00 mmol) in THF (40 mL) resulted in precipitation of a white solid and formation of a pink solution. The solvent was removed under vacuum and hexane added (30 mL). The mixture was then warmed and filtered. The filtrate was concentrated to ca. 25 mL affording X-ray quality pink crystals of **4b** (0.36 g, 61%). IR (Nujol): $\tilde{\nu}$ = 1593 s, 1563 w, 1318 w, 1291 s, 1277 m, 1242 s, 1210 w, 1158 s, 1116 vs, 1051 m, 1001 s, 916 vs, 843 vs, 822 s, 788 m, 768 m, 729 vs, 679 m, 626 s, 597 s cm⁻¹. C₄₀H₆₄Cl₂Er₂N₄O₄Si₄ (1182.73): calcd. C 40.62, H 5.45, N 4.74; found C 39.79, H 5.54, N 4.96.

[Tb(L¹)₂(μ-Cl)]₂ (4c): A similar preparation method to that used for compound **4a** gave large pale yellow crystals of **4c** (0.40 g, 68%). IR (Nujol): $\tilde{\nu}$ = 1593 s, 1563 w, 1504 s, 1320 w, 1293 s, 1265 s, 1240 s, 1210 w, 1158 s, 1115 vs, 1051 m, 1001 s, 914 vs, 842 vs, 826 sh w, 783 m, 766 m, 727 vs, 669 m, 625 s, 596 s cm⁻¹. C₄₀H₆₄Cl₂N₄O₄Si₄Tb₂ (1166.06): calcd. C 41.20, H 5.53, N 4.80; found C 41.42, H 5.39, N 4.76.

[Nd(L²)₂(μ-Cl)]₂(PhMe)₂ [5a·(PhMe)₂]: [Li(L²)(DME)] (0.72 g, 2.00 mmol) was added to a stirred solution of [NdCl₃(THF)₂] (0.40 g, 1.00 mmol) in THF (40 mL). The resulting blue solution was evaporated to dryness and toluene was added (30 mL). The reaction mixture was filtered and the filtrate volume was reduced

under vacuum (ca.15 mL). Upon standing overnight single blue crystals suitable for X-ray crystallography formed (0.35 g, 72%). IR (Nujol): $\tilde{\nu}$ = 1585 s, 1294 s, 1266 m, 1243 s, 1185 s, 1160 s, 1100 s, 1074 w, 1036 m, 1022 w, 936 vs, 859 m, 828 br. s, 774 m, 746 s, 727 s, 690 s, 679 w, 623 w cm⁻¹. Vis/near IR (DME): λ_{max} (ε) = 527 (55), 586 (75), 755 (25), 811 (28), 885 (22) nm (dm³ mol⁻¹). ¹H NMR (300 MHz, C₆D₆, 298 K): δ = -8.73 (br. s, 8 H, H-2',H-6'), -5.04 (br. s, 36 H, SiMe₃), 0.08 (s, 8 H, H-3',H-5'), 1.18 (s, 4 H, H-4'), 1.49 (br. s, 8 H, H-4, H-5), 2.10 (s, 6 H, PhMe), 7.02-7.20 (m, 10 H, PhMe), 15.4 (br. s, 4 H, H-3 or H-6), 30.95 (br. s, 4 H, H-3 or H-6). C₇₄H₈₈Cl₂N₄Nd₂O₄Si₄ (1569.22): calcd. C 54.64, H 5.65, N 3.57; found C 54.47, H 5.53, N 3.63.

[Li(L¹)(OEt₂)₂]: *n*BuLi (32 mL, 0.05 mol) was added dropwise to a stirred solution of L¹H (0.05 mol, 10 g) in Et₂O (80 mL) at 0 °C, and the resulting solution was warmed to room temperature over ca. 1 h. The resulting white precipitate was cooled to -78 °C, washed with hexane (40 mL) and dried under vacuum (11.9 g, 86%). A small amount of [Li(L¹)(OEt₂)₂] was redissolved in Et₂O whereupon light-sensitive colourless crystals of good X-ray quality formed. IR (Nujol): $\tilde{\nu}$ = 1585vs, 1558s, 1280s, 1239s, 1212s, 1171s, 1117vs, 1052s, 1029vs, 934s, 840s, 821s, 734vs, 660s, 594s cm⁻¹. MS: *m/z* (%) = 201 (100) [LiL¹]⁺, 195 (25) [L¹H]⁺, 165 (60) [L¹H - 2Me]⁺, 150 (25) [L¹H - 3Me]⁺, 135 (20) [C₆H₅ONSi]⁺, 73 (40) [SiMe₃]⁺, 58 (20) [SiMe₂]⁺. ¹H NMR (300 MHz, C₇D₈, 298 K): δ = 0.11 (s, 18 H, SiMe₃), 1.04 [t, ³J = 7.0 Hz, 12 H, Me (OEt₂)], 3.26 [q, ³J = 7.0 Hz, 8 H, CH₂ (OEt₂)], 3.35 (s, 6 H, OMe), 6.50-6.57 (dd, ³J = 7.2, ⁴J = 1.6 Hz, 2 H, H-6), 6.62-6.68 (td, ³J = 7.0, ⁴J = 1.5 Hz, 2 H, H-5), 6.85-6.95 (td, ³J = 7.0, ⁴J = 1.6 Hz, 2 H, H-4), 6.96-7.04 (dd, ³J = 7.2, ⁴J = 1.7 Hz, 2 H, H-3). ⁷Li NMR (155.51 MHz, C₇D₈, 298 K): δ = 1.85. C₂₈H₅₂Li₂N₂O₄Si₂ (550.79) (solvate): calcd. C 61.06, H 9.52, N 5.09. C₁₀H₁₆LiNOSi (201.27) (LiL²): calcd. C 59.68, H 8.01, N 6.96; found C 58.92, 59.08, H 8.84, 8.67, N 5.82, 6.01.

Structure Determinations: Data for the crystallographic structure determinations of compounds **1e**, **2a**·(PhMe), **2d** and **2e** are given in Table 5 while similar data for **4a-4c**, **5a**·(PhMe)₂ and [Li(L¹)-

Table 6. Crystallographic and refinement parameters for [Ln(L)₂(μ-Cl)]₂ and [Li(L¹)(OEt₂)₂] complexes

Compound	[Yb(L ¹) ₂ (μ-Cl)] ₂ 4a	[Er(L ¹) ₂ (μ-Cl)] ₂ 4b	[Tb(L ¹) ₂ (μ-Cl)] ₂ 4c	[Nd(L ²) ₂ (μ-Cl)] ₂ ·(PhMe) ₂ 5a ·(PhMe) ₂	[Li(L ¹)(OEt ₂) ₂]
Empirical formula	C ₄₀ H ₆₄ Cl ₂ N ₄ O ₄ Si ₄ Yb ₂	C ₄₀ H ₆₄ Er ₂ Cl ₂ N ₄ O ₄ Si ₄	C ₄₀ H ₆₄ Cl ₂ N ₄ O ₄ Si ₄ Tb ₂	C ₇₄ H ₈₈ Cl ₂ N ₄ Nd ₂ O ₄ Si ₄	C ₂₈ H ₅₂ Li ₂ N ₂ O ₄ Si ₂
Molecular Weight	1194.3	1182.73	1166.06	1569.22	550.78
Crystal system	monoclinic	monoclinic	monoclinic	triclinic	triclinic
Space Group	<i>P</i> 2 ₁ / <i>n</i>	<i>P</i> 2 ₁ / <i>n</i>	<i>P</i> 2 ₁ / <i>n</i>	<i>P</i> 1bar	<i>P</i> 1bar
Crystal size [mm]	0.15 × 0.15 × 0.10	0.23 × 0.23 × 0.18	0.25 × 0.18 × 0.13	0.25 × 0.20 × 0.13	0.30 × 0.13 × 0.13
<i>a</i> [Å]	14.6143(3)	14.6389(1)	14.5575(1)	10.1897(1)	9.9320(5)
<i>b</i> [Å]	18.0518(4)	18.1148(1)	18.2621(2)	13.3375(2)	10.0400(5)
<i>c</i> [Å]	19.0058(5)	19.0169(2)	19.0461(2)	15.5566(2)	10.4465(4)
α [deg]	90	90	90	74.48(3)	117.651(3)
β [deg]	92.327(1)	92.875(1)	92.653(1)	77.36(3)	94.472(3)
γ [deg]	90	90	90	67.38(3)	111.482(2)
<i>V</i> [Å ³]	5009.9(17)	5036.6(17)	5058.0(18)	1848.0(6)	818.9(3)
<i>Z</i>	4	4	4	1	1
<i>d</i> _{calcd} (g cm ⁻³)	1.583	1.560	1.531	1.410	1.117
<i>F</i> (000)	2376	2360	2336	802	300
μ(Mo- <i>K</i> _α) (mm ⁻¹)	3.953	3.550	3.013	1.575	0.140
2θ _{max} (°)	56.6	56.6	56.6	56.6	56.5
<i>N</i> , <i>N</i> _o	12341, 6357	12025, 8910	12457, 9175	8040, 7457	3887, 2831
<i>Goof</i>	1.033	1.025	1.039	1.049	1.047
<i>R</i> , <i>R</i> _w (observed data)	0.0686, 0.1023	0.0308, 0.0667	0.0369, 0.0728	0.0250, 0.0552	0.0589, 0.1394
<i>R</i> , <i>R</i> _w (all data)	0.1795, 0.1272	0.0545, 0.0734	0.0639, 0.0803	0.0292, 0.0567	0.0912, 0.1541

(OEt₂)₂ are listed in Table 6. Data for **2a**·(C₅H₉Me) and **2b**·(C₅H₉Me) are provided in CCDC-174206/174207. Crystals were mounted in an inert atmosphere under viscous oil onto a glass fibre. Low-temperature (≈123 K) data were collected on an Enraf–Nonius CCD area-detector diffractometer (Mo-K_α radiation, λ 0.71073 Å, frames comprised 1.0° increments in φ and ω yielding a sphere of data) with proprietary software (Nonius B.V., 1998). Each data set was merged (*R*_{int} as quoted) to *N* unique reflections; the structures were solved by conventional methods and refined with anisotropic thermal parameter forms for the non-hydrogen atoms by full-matrix least-squares on all *F*² data using SHELX 97 software package.^[58] Hydrogen atoms were included in their calculated positions and allowed to ride on the parent carbon atom with isotropic thermal parameters. For **2a**·(C₅H₉Me) and **2b**·(C₅H₉Me), the lattice solvent was also modelled as PhMe, disordered PhMe, or THF, and in each case the refinement was unstable by contrast with C₅H₉Me, the presence of which was also indicated by the NMR spectrum of **2b**. CCDC-174197 to CCDC-174207 contain the supplementary crystallographic data for this paper. These data can be obtained free of charge at www.ccdc.cam.ac.uk/conts/retrieving.html [or from the Cambridge Crystallographic Data Centre, 12, Union Road, Cambridge CB2 1EZ, UK; Fax: (internat.) +44-1223/336-033; E-mail: deposit@ccdc.cam.ac.uk].

Acknowledgments

We gratefully acknowledge support of this work from the Australian Research Council and Australian Postgraduate and Monash Postgraduate Publication Awards to N. M. S.

- [1] G. B. Deacon, C. M. Forsyth, N. M. Scott, B. W. Skelton, A. H. White, *Aust. J. Chem.* **2001**, *7*, 439–446.
- [2] S. Gambarotta, J. Jubb, J. Song, D. Richeson, *Zirconium and Hafnium Complexes in Oxidation State +4, Chap. 11*, in *Comprehensive Organometallic Chemistry II* (Eds.: E. W. Abel, F. G. A. Stone, G. Wilkinson), Pergamon, Oxford, U. K., **1995**, *4*.
- [3] A. N. Guram, R. F. Jordan, *Cationic Organozirconium and Organohafnium Complexes, Chap. 12*, in *Comprehensive Organometallic Chemistry II* (Eds.: E. W. Abel, F. G. A. Stone, G. Wilkinson), Pergamon, Oxford, U. K., **1995**, *4*.
- [4] H. Schumann, J.-A. Meese-Markscheffel, L. Esser, *Chem. Rev.* **1995**, *95*, 865–986.
- [5] F. T. Edelmann, *Scandium, Yttrium, Lanthanides and Actinides*, Chap. 2 in *Comprehensive Organometallic Chemistry II* (Eds.: E. W. Abel, F. G. A. Stone, G. Wilkinson), Pergamon, Oxford, U. K., **1995**, *4*, 11.
- [6] M. N. Bochkarev, L. N. Zakharov, G. S. Kalinina, *Organoderivatives of Rare Earth Elements*, Kluwer Academic Publishers, Dordrecht/Boston/London, **1995**.
- [7] R. Anwender, *Top. Organomet. Chem.* **1999**, *2*, 1–61.
- [8] A. Togni, L. M. Venanzi, *Angew. Chem. Int. Ed. Engl.* **1994**, *33*, 497–526.
- [9] R. Kempe, *Angew. Chem. Int. Ed.* **2000**, *39*, 468–493.
- [10] F. T. Edelmann, *Coord. Chem. Rev.* **1995**, *137*, 403–481.
- [11] W. J. Evans, M. A. Ansari, J. W. Ziller, S. I. Khan, *Inorg. Chem.* **1996**, *35*, 5435–5444.
- [12] L. G. Hubert-Pfalzgraf, *Coord. Chem. Rev.* **1998**, *178–180*, 967–997.
- [13] R. C. Mehrotra, A. Singh, U. M. Tripathi, *Chem. Rev.* **1991**, *91*, 1287–1303.
- [14] D. C. Bradley, R. C. Mehrotra, I. P. Rothwell, A. Singh, *Alkoxo and Aryloxo Derivatives of Metals*, Academic Press, London, **2001**.
- [15] D. C. Bradley, M. B. Hursthouse, H. C. Aspinall, K. D. Sales, N. P. C. Walker, B. Hussain, *J. Chem. Soc., Dalton Trans.* **1989**, 623–626.
- [16] D. C. Bradley, M. B. Hursthouse, H. C. Aspinall, K. D. Sales, N. P. C. Walker, *J. Chem. Soc., Chem. Commun.* **1985**, 1585–1586.
- [17] M. Karl, G. Seybert, W. Massa, S. Agarwal, A. Greiner, K. Dehnicke, *Z. Anorg. Allg. Chem.* **1999**, *625*, 1405–1407.
- [18] J. Collin, N. Giuseppone, N. Jaber, A. Domingos, L. Maria, I. Santos, *J. Organomet. Chem.* **2001**, *628*, 271–274.
- [19] F. T. Edelmann, *J. Alloys and Compounds* **1994**, *207/208*, 182–188.
- [20] J. A. R. Schmidt, J. Arnold, *Chem. Commun.* **1999**, 2149–2150.
- [21] R. Duchateau, C. T. van Wee, J. H. Teuben, *Organometallics* **1996**, *15*, 2291–2302.
- [22] P. W. Roesky, *Chem. Ber./Recueil* **1997**, *130*, 859–862.
- [23] P. W. Roesky, M. R. Bürgstein, *Inorg. Chem.* **1999**, *38*, 5629–5632.
- [24] H. Görls, B. Neumüller, A. Scholz, J. Scholz, *Angew. Chem.* **1995**, *107*, 732–735; *Angew. Chem. Int. Ed. Engl.* **1995**, *34*, 673–676.
- [25] R. Duchateau, T. Tumstra, E. A. C. Brussee, A. Meetsma, P. T. van Duijnen, J. H. Teuben, *Organometallics* **1997**, *16*, 3511–3522.
- [26] R. Anwender, *Top. Curr. Chem.* **1996**, *179*, 33–112.
- [27] G. B. Deacon, C. M. Forsyth, P. C. Junk, B. W. Skelton, A. H. White, *J. Chem. Soc., Dalton Trans.* **1998**, 1381–1387.
- [28] G. B. Deacon, C. M. Forsyth, N. M. Scott, *Eur. J. Inorg. Chem.* **2000**, 2501–2506.
- [29] G. B. Deacon, C. M. Forsyth, N. M. Scott, *J. Chem. Soc., Dalton Trans.* **2001**, 2494–2501.
- [30] C. J. Pouchert, J. R. Campbell, *Aldrich Library of NMR Spectra*, Aldrich Chemical Company, Milwaukee, Wisconsin, **1974**, *1*, 32C.
- [31] W. T. Carnall, *The Absorption and Fluorescence Spectra of Rare Earth Ions in Solution*, in *Handbook on the Physics and Chemistry of Rare Earths*, North-Holland, Amsterdam, **1979**, *3*, 171.
- [32] M. Johnson, J. C. Taylor, G. W. Cox, *J. Appl. Crystallogr.* **1980**, *13*, 188–189.
- [33] R. D. Shannon, *Acta Crystallogr., Sect. A* **1976**, *32*, 751–767.
- [34] G. B. Deacon, P. I. MacKinnon, T. W. Hambley, J. C. Taylor, *J. Organomet. Chem.* **1983**, *259*, 91–97.
- [35] G. B. Deacon, T. Feng, P. C. Junk, B. W. Skelton, A. N. Sobolev, A. H. White, *Aust. J. Chem.* **1998**, *51*, 75–89.
- [36] A. Recknagel, A. Steiner, S. Brooker, D. Stalke, F. T. Edelmann, *J. Organomet. Chem.* **1991**, *415*, 315–326.
- [37] R. A. Andersen, D. H. Templeton, A. Zalkin, *Inorg. Chem.* **1978**, *17*, 2317–2319.
- [38] P. G. Eller, D. C. Bradley, M. B. Hursthouse, D. W. Meek, *Coord. Chem. Rev.* **1977**, *24*, 1–95.
- [39] H. Schumann, J. Winterfeld, E. C. E. Rosenthal, H. Hemling, L. Esser, *Z. Anorg. Allg. Chem.* **1995**, *621*, 122–130.
- [40] R. K. Minhas, Y. Ma, J.-I. Song, S. Gambarotta, *Inorg. Chem.* **1996**, *35*, 1866–1873.
- [41] M. Wedler, F. Knösel, U. Pieper, S. Dietmar, F. T. Edelmann, H.-D. Amberger, *Chem. Ber.* **1992**, *125*, 2171–2181.
- [42] A. Recknagel, F. Knösel, H. Gornitzka, M. Noltemeyer, F. T. Edelmann, U. Behrens, *J. Organomet. Chem.* **1991**, *417*, 363–375.
- [43] S. Arndt, P. Voth, T. P. Spaniol, J. Okuda, *Organometallics* **2000**, *19*, 4690–4700.
- [44] H. Lueken, J. Schmitz, W. Lamberts, P. Hannibal, K. Handrick, *Inorg. Chim. Acta* **1989**, *156*, 119–124.
- [45] H. Schumann, M. R. Keitsch, J. Demtschuk, G. A. Molander, *J. Organomet. Chem.* **1999**, *582*, 70–82.
- [46] W. J. Evans, D. K. Drummond, J. Grate, H. Zhang, J. L. Atwood, *J. Am. Chem. Soc.* **1987**, *109*, 3928–3936.
- [47] G. B. Deacon, T. Feng, S. Nickel, B. W. Skelton, A. H. White, *J. Chem. Soc., Chem. Commun.* **1993**, 1328–1329.
- [48] B. Cetinkaya, P. B. Hitchcock, M. F. Lappert, M. C. Misra, A. J. Thorne, *J. Chem. Soc., Chem. Commun.* **1984**, 148–149.

- [49] M. F. Lappert, M. J. Slade, A. Singh, J. L. Atwood, R. D. Rogers, R. Shakir, *J. Am. Chem. Soc.* **1983**, *105*, 302–304.
- [50] J. R. van den Hende, P. B. Hitchcock, S. A. Holmes, M. F. Lappert, S. Tian, *J. Chem. Soc., Dalton Trans.* **1995**, 3933–3939.
- [51] J. Marcalo, A. P. De Matos, *Polyhedron* **1989**, *8*, 2431–2437.
- [52] B. Fan, Q. Shen, Y. Lin, *J. Organomet. Chem.* **1989**, *377*, 51–58.
- [53] G. B. Deacon, T. Feng, C. M. Forsyth, A. Gitlits, D. C. R. Hockless, Q. Shen, B. W. Skelton, A. H. White, *J. Chem. Soc., Dalton Trans.* **2000**, 961–966.
- [54] L. M. Engelhardt, G. E. Jacobsen, P. C. Junk, C. L. Raston, B. W. Skelton, A. H. White, *J. Chem. Soc., Dalton Trans.* **1988**, 1011–1020.
- [55] F. A. Cotton, S. C. Haefner, J. H. Matonic, X. Wang, C. A. Murillo, *Polyhedron* **1997**, *16*, 541–550.
- [56] J. L. Atwood, W. E. Hunter, A. L. Wayda, W. J. Evans, *Inorg. Chem.* **1981**, *20*, 4115–4119.
- [57] G. Meyer, *Binary Lanthanoid(III) Halides, MX₃ (X = Cl, Br, I)*, in *Syntheses of Lanthanoid and Actinide Compounds* (Eds.: G. Meyer, L. R. Morss), Kluwer, Dordrecht, **1991**.
- [58] G. M. Sheldrick, *SHELX97, Program for Crystal Structure Determination*, Universität Göttingen, **1997**.

Received November 16, 2001
[101461]